A Cooperative Resilience-Oriented Planning Framework for Integrated Distribution Energy Systems and Multi-Carrier Energy Microgrids Considering Energy Trading

Sabzpoosh Saravi, Seyed Vahid; Kalantar, Mohsen; Anvari-Moghaddam, Amjad

Published in:
Sustainable Cities and Society

DOI (link to publication from Publisher):
10.1016/j.scs.2023.105039

Publication date:
2024

Document Version
Publisher's PDF, also known as Version of record

Sustainable Cities and Society 100 (2024) 105039

Contents lists available at ScienceDirect

Sustainable Cities and Society

journal homepage: www.elsevier.com/locate/scs

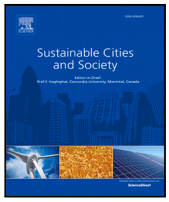

A cooperative resilience-oriented planning framework for integrated distribution energy systems and multi-carrier energy microgrids considering energy trading

Vahid Sabzpoosh Saravi [a], Mohsen Kalantar [a], Amjad Anvari-Moghaddam [b,*]

[a] Department of Electrical Engineering, Iran University of Science and Technology, Tehran, Iran
[b] Department of Energy (AAU ENERGY), Aalborg University, 9220 Aalborg, Denmark

ARTICLE INFO

Keywords:
Integrated energy systems
Multi-carrier energy microgrid
Resilience-oriented planning
Cooperative planning framework
DC power distribution system

ABSTRACT

Integrated distribution systems (IDSs) and multi-carrier energy microgrids (MCEMs) can play a crucial role in enhancing distribution energy systems' overall efficiency and flexibility. By cascading energy usage and cooperating through energy trading, IDSs and MCEMs can reduce overall system costs and provide more flexibility for system operators. Adding resilience to the planning problem of IDSs can reduce planning costs in the long term, as proactive preparedness is key to coping with high-impact rare (HR) events. Adding resilience to the planning problem of IDSs can reduce the planning costs in the long term since proactive preparedness is a key necessity to cope with high-impact rare (HR) events. This paper proposes a resilience-oriented stochastic tri-level and two-stage cooperative expansion planning of IDSs and MCEMs, considering energy trading between IDSs and MCEMs. The first stage comprises two levels; the first level minimizes the investment and operation costs of IDSs and MCEMs, while the second level desires to maximize the energy exchange profit for MCEMs and thus reduce the overall costs. The second stage includes the third level problem involving two objective functions: resilience cost minimization and resilience index (RI) maximization. The multi-objective problem in the second stage is converted into a single-objective problem using the min–max regret method. The DC and AC configurations for the power distribution system (PDS) and power microgrids (PMGs) are studied to identify the optimal configuration of these networks in the expansion planning problem. A new framework is proposed based on an aggregator-agent splitting solution using the aggregator coupling coordinator unit (ACC) responsible for coordinating IDNs and MCEMs. The studied large-scale complex optimization problem is efficiently solved computationally by introducing a combined adaptive dynamic programming (ADP) and linearized alternating direction method of multipliers with parallel splitting (LADMMPSAP) algorithm. Three cases are studied to demonstrate the effectiveness of the proposed model and method. The results depict that MCEMs help reduce expansion planning costs and improve the system's resilience. Adding resilience to the expansion planning problem enhances the resilience of the whole system and simultaneously reduces the costs by 2.7%. The expansion planning costs for the AC and DC configuration are close, and the AC is the optimal choice in all case studies. By increasing the planning horizon from 5 to 10 years, DC will be the optimal solution since network reinforcement costs and power losses are significantly lower.

1. Introduction

The choice of policy, technology, and economics are the main levers to expand the energy systems and positively contribute to the future energy system's evolution. In this regard, the need for rethinking current policies and principles of energy system planning is highlighted. Efficient planning of energy systems can have benefits, such as increasing efficiency, reducing the need for investment, and reducing pollution. Increasing energy system couplings and interaction among electricity, gas, and thermal energy carriers inspire the integrated energy systems (IESs) concept (Geidl & Andersson, 2007). IESs at different levels (district, city, or country) demonstrate technical, economic, and environmental advantages over independent energy systems (Geidl & Andersson, 2007; Mancarella, 2014). The multi-period multi-energy scheduling is a challenging optimization problem because of its solid couplings and inherent non-convexities within IESs. Authors of Zhang et al. (2015) have proposed an IES expansion planning model based

* Corresponding author.
E-mail addresses: vahid_Sabzpoosh@elec.iust.ac.ir (S. Sabzpoosh Saravi), kalantar@iust.ac.ir (M. Kalantar), aam@energy.aau.dk (A. Anvari-Moghaddam).

https://doi.org/10.1016/j.scs.2023.105039
Received 14 June 2023; Received in revised form 29 September 2023; Accepted 4 November 2023
Available online 15 November 2023

Nomenclature

Indices

T	Index of planning period
T^g, T^s, T^L	Indices of generation, storage and, line useful lifetime
$y, \mathbb{S}, t$	Indices of years, seasons, and time
g, s, L	Indices of generation, storage units and lines
i, j	Indices of PDS and PMGs buses
k, l	Indices of GDS and GMGs nodes
m, r	Indices of DHS and HMGs nodes
$\hat{i}, \hat{k}, \hat{m}$	Indices of coupling buses between agents
N	Index of energy agents (IDSs and MCEMs)
v	Index of wind speed profile

Symbols

$\underline{\cdot}, \overline{\cdot}$	Symbols for lower and upper limits

Sets

$Y, \Omega_{\mathbb{S}}$	Sets of the planning years and seasons
T_d	Set of daily load periods in seasons
T_e	Set of emergency load periods in years
Ω_N^n, Ω_N^L	Sets of buses/nodes and lines in the agents
Ω_N^g, Ω_N^s	Sets of generation and storage units
$\Omega_N^{slack}, \Omega_N^{Co}$	Sets of slack and coupling buses/nodes
$\overline{S}^{Imp}$	Maximum imported apparent power from upstream power grid
N^{FP}	Number of failed power poles
L^{FC}	Lengths of failed conductors
ψ_{kl}, ψ_{mr}	Weymouth constant for gas and heat pipelines
φ_{mr}	Heat loss coefficient of heat pipelines
ζ_{kl}	Compression coefficient in active gas pipelines
ω_N	The importance weight of agent N
Θ_{ξ}	Probability of scenario ξ
K^{vsc}, M^{vsc}	Converter constant value and modulation index of VSCs
η^{vsc}	Conversion efficiency of VSCs

Variables

$P_{i,g,t}, Q_{i,g,t}$	Active and reactive power generation of generator g at bus i at time t
$P_{i,s,t}^{ch}, P_{i,s,t}^{dis}$	Charge and discharge power of storage s
$P_{i,t}^{DR}, Q_{i,t}^{DR}$	Active and reactive curtailed power by DRP
$P_{i,t}^{inj}, Q_{i,t}^{inj}$	Injected active and reactive power at bus i
$P_{ij,t}, Q_{ij,t}$	Active and reactive flow in line ij
$P_{i,t}^{ex}$	The exchanged power with coupled energy agents
$\Omega_{DS}^f, \Omega_{MG}^f$	Sets of the PDS and PMGs damaged lines

Parameters

G^y, B^y	Real and imaginary parts of admittance matrix
$P_{i,t}^{Sh}$	Upper limit for demand shedding in power energy agents
$q_{i,t}^{Sh}, M_{i,t}^{Sh}$	Upper limit for demand shedding in gas, and heat energy agents
$P_{i,t}^D, Q_{i,t}^D$	Active and reactive power demands
$q_{k,t}^D, M_{m,t}^D$	Gas and heat demands
$\underline{CR}, \overline{CR}$	Lower and upper limits of compressor compression ratio
$\eta_{N,s}^{ch}, \eta_{N,s}^{dis}$	Charge and discharge efficiency of storage units
$\overline{P}_{ij}^{loss}$	Upper limit for active power loss of line
$\overline{E}_{N,s}$	Capacity of energy storage units
Δt	Duration of each time period
P_{Th}^f	Failure probability thresholds
$k_1 - k_6$	Energy conversion coefficients
τ^a	Ambient temperature
$IC_{N,g}, IC_{N,s}$	Investment costs of generation and storage units
$IC_{N,L}, IC_{N,L}^{(r)}$	Investment and reinforcement costs of lines
C^{Budget}	Annual budget
C^{Loss}	Cost of electrical energy loss in $\$/MWh$
C_N^{LL}	Value of lost load in $\$/MWh$
$P_{N,y,\mathbb{S},t}^{loss}$	PDS and PMGs power losses
$V_{i,t}, \theta_{i,t}$	Voltage magnitude and angle of bus i
P_t^{Imp}, Q_t^{Imp}	Imported active and reactive power to upstream grid
$q_{k,g,t}, m_{m,g,t}$	Gas and water flow of source g
$q_{k,s,t}^{ch}, q_{k,s,t}^{dis}$	Charge and discharge flow of GS s at node k
$q_{kl,t}, m_{mr,t}$	Gas and water flow in pipelines kl and mr
$q_{k,t}^{DR}, M_{m,t}^{DR}$	Gas and heat curtailed demand by DRP
$q_{k,t}^{ex}, M_{m,t}^{ex}$	The exchanged gas and heat with coupled energy agents
$\Gamma_{k,t}, \Pi_{m,t}$	Gas and water pressure at nodes k and m
$M_{m,g,t}$	Heat generation of source g at node m
$M_{m,s,t}^{ch}, M_{m,s,t}^{dis}$	Charge and discharge flow of TS
$\tau_{mr,t}^{in}, \tau_{mr,t}^{out}$	Inlet and outlet temperature of pipeline mr
$\tau_{m,t}^{mix}$	Mixed temperature of node m
$P_{\hat{i},t}^{P2G}, P_{\hat{i},t}^{EB}$	Power consumption of P2G and EB
$q_{\hat{k},t}^{GB}, q_{\hat{k},t}^{CHP}$	Gas consumption of GB and CHP
$P_{k,t}^{GC}, P_{H,m,t}^{WP}$	Power consumption of GC, and WP
$SoC_{N,s,t}$	State of charge in storage s
$E_{N,t}^S, E_{N,,t}^P$	Sold and purchased power/heat/gas
$\Pi_{N,t}^S, \Pi_{N,t}^P$	Sell and purchase price (per unit) of power/gas/heat

on the energy hub (EH), considering combined heat and power units (CHPs) and gas boilers (GBs). Design and operation of park-level IESs considering the different climate zones in China is proposed in Zhao et al. (2023). A two-stage optimization approach is presented in which total cost minimization is done in the first stage, and the resulting operation scenarios are used to optimize the operation cost in the second stage. An energy management model for the IES, including power, water, and gas systems networked with EHs, has been proposed in Zhao et al. (2021), which focuses on minimizing the operation costs of the IES. In Zhang et al. (2014), CHP unit allocation in the integrated power distribution system (PDS) and gas distribution system (GDS) is optimized to maximize the power and heat supply for satisfying flexible consumer needs. An IES scheduling model based on energy hubs as distributed decision-makers has been investigated in Xu, Wu, et al. (2020), which creates synergic coupling for power, heat, and natural gas networks. This model solves the mixed-integer second-order

$C^{rep}_{pole}, C^{rep}_{con}$	Repair cost of failed power poles and line conductors
$C^{RTP}_{N,y,\mathbb{S},t}$	Real-time price of energy in agent N
$x_{N,L,t}, x^{r}_{N,L,t}$	Binary variables for investment and reinforcement of lines
C^{CEP}, C^{RI}	Total coordinated expansion planning and resilience costs
C^{Pr}	Profit of energy exchange
$x^{ch}_{N,s,t}$	Statuses of storage units; charge (1), discharge (0)
$x_{N,g,t}, x_{N,s,t}$	Binary variables for generation and storage units investment
$C^{Inv}_{\xi}, C^{Op}_{\xi}$	Investment and operation costs in scenario ξ
OC^{F}, OC^{V}	Fixed and variable operational costs

cone programming optimization problem to optimize the operation of coupled networks over a 24-hour scheduling period. A continuous-time model for integrated electricity and district heating networks considering wind generation uncertainty is proposed in Nourollahi et al. (2023). The paper concludes that integrated power and district heating networks with energy storage devices can provide flexibility services in power system operation and enhance the reliability and cost-effectiveness of the system. An operation cost minimization model for integrated power, gas, and district heating systems considering multi-carrier energy storage technologies is developed in Mirzaei et al. (2020). The paper investigated the role of multi-carrier storage technologies in operation cost decreases. A two-stage planning framework for distributed energy networks is proposed in Ren et al. (2023), which includes a variety of energy sources trade to explore the possible benefits. The energy storage and transmission equipment with two scheduling strategies are developed with different priorities to balance supply and demand in the energy system. The first stage maximizes the system's economic, energetic, and environmental performance, while the second stage determines the optimum energy trading prices. A daily energy management model for energy hubs using robust optimization considering power-to-gas (P2G) and CHP technologies is proposed in Habibifar et al. (2021). The main objective of the model is to capture the electricity price variation with no information to help minimize operation costs. The concept of distribution system resilience against high-impact rare (HR) events has attracted wide attention in recent years since it can cause extended energy supply disruption and severe socio-economic losses. For example, there were 20 natural disasters in the US, each incurring losses surpassing $1 billion in 2021 (Poudyal et al., 2022). Few works have attempted to enhance the resilience of IESs in a long-term planning problem. Proactive preparedness by considering incorporating resilience in system planning is a sensible approach for integrated distribution systems (IDSs) to diminish these losses. Authors of Salyani et al. (2023) proposed a resilience-oriented scheduling framework using a cooperative game approach for transactive MGs. These MGs engage in energy transactions through a local market. The paper aims to minimize the operational costs of MGs under normal conditions while ensuring that MGs can serve their loads during emergency conditions. The paper focuses solely on the operational view and does not consider the improvement of resilience from long-term planning aspects. A resilience-oriented proactive scheduling method to enhance the preparedness of multi-carrier energy microgrids (MCEMs) against an ongoing hurricane for integrated gas and power distribution systems is discussed in Amirioun et al. (2019). An MCEM is a small-scale distributed energy system capable of operating independently from the main distribution system. It can incorporate distributed power, gas, heat sources, and energy storage systems. Additionally, MCEMs maintain the ability to exchange energy with the upstream distribution energy system. This allows them to consume energy from the grid when needed efficiently and supply any excess energy back to the grid. As a result, MCEMs offer heightened flexibility and resilience in managing energy resources. Authors of Tabebordbar et al. (2023) proposed a reliability-oriented optimal sizing method for integrated power and gas networks, which determines the optimal size of the CHP and P2G as the first-rate options to integrate a power network to a natural gas network. A reliability method for IESs is proposed in Zhao et al. (2022). The fault incidence matrix method is used to analytically evaluate the impact of equipment failure on the system energy supply, which can demonstrate the critical systems with the most effect on the energy system reliability. The reliability constraints are added to the proposed model in He et al. (2018) for planning coupled PDS and GDS. The solution guarantees the desired reliability requirement for PDS. An interactive framework for integrated power-water distribution systems utilizing a stochastic energy management program for microgrids (MGs) connected to PDS is outlined in Najafi et al. (2019, 2020). The introduced model tries to improve the resilience of IDSs against natural disasters. An expansion planning model that considers the integration of distributed generators to PDS is proposed in Behzadi and Bagheri (2023), which includes investment, operational, emissions, and resilience costs. The model aims to minimize costs while enhancing resilience by formation of MGs utilizing tie-lines for reconfiguration. The optimal siting and sizing of DGs and substations are considered configuring resilient MGs capable of withstanding extreme weather events adequately. A resilience-oriented model for MG formation in the integrated power and gas networks is proposed in Hemmati et al. (2021). A cost and resilience minimization objective function is proposed, which tries to improve the system resilience and reduce the operation cost by optimal sizing and sitting of CHPs. Critical load restoration is defined to evaluate the resilience of the system. A two-stage resilience-constrained model for the MCEMs using mixed-integer quadratic programming is proposed in Gharehveran et al. (2022). The investment decisions are taken in the first stage, while the operation variables are optimized in the second stage with the aim of resilience improvement. A resilience-oriented two-stage stochastic chance-constrained model for IESs considering an integrated demand response program (DRP) is proposed in Guo et al. (2019). The expected energy not supplied (EENS) has been chosen as the reliability criterion. Authors of Bao et al. (2020) proposed a framework for evaluating the resilience of IESs, including natural gas system, power system, and EHs under a wind storm. Nodal resilience metrics for energy subsystems are introduced, which include expected energy losses, collapse ratio, and recovery ratio. A co-optimization model for an integrated electricity–gas–heat urban energy system considering resilience enhancement during extreme events is proposed in Tao et al. (2023). The model aims to enhance the resilience of IESs by considering weighted load shedding, the comfort of heat customers, and the time delay of data centers. Various measures are considered to enhance resilience, including redistributing workloads, reusing waste heat, co-optimizing multiple energy systems, dispatching repair crews, and utilizing linepack storage. Ultimately, the paper concludes that the configuration of BESSs and the efficient dispatching of repair crews play a vital role in ensuring optimal system performance. Authors of Faramarzi et al. (2023) introduced a three-stage hybrid framework to address the resilience-oriented distribution network planning problem. In the first stage, the decision-making process focuses on line hardening and distributed generation placement, which aims to enhance the overall resilience of the distribution network. In the second stage, the paper discusses emergency and normal operation optimization. The impact of potential hurricanes is specifically evaluated in post-event emergency operation conditions using a worst-case scenario approach. Normal operation conditions are assessed using a scenario-based stochastic approach. The third stage proposes a risk-averse hardening re-plan strategy using the information gap decision

theory. A resilience-oriented planning approach for PDS using a three-stage hybrid stochastic-robust model is proposed in Wang and Bo (2023). Investment in renewable energy sources and power lines in the first stage, reinvestment in urgent mobile storage renting and line hardening in the second stage, and daily system operations and emergent scenarios in the third stage are modeled. Integration of other distribution systems or MCEMs is not considered. The paper focuses on data centers as the power consumption subject that couples electricity, cooling, and heating energy sources. However, the uncertainties are not considered. A two-stage mixed integer linear programming (MILP) model for optimizing the configuration of MESs at the planning stage is proposed in Huang et al. (2019). The paper models IES as a directed acyclic graph with multiple layers based on energy hubs. Resilience-oriented planning for MGs utilizing deep learning techniques is investigated in Vilaisarn et al. (2022). A stochastic bilevel model is proposed to minimize the operational costs of MGs and maximize their resilience by identifying the optimal location of distributed energy resources (DERs) and isolating switches in the PDS. An optimal planning for a park-integrated energy system for PDS considering resilience by utilizing a quantified index for resilience assessment is proposed in Liu et al. (2021). The entropy is used to reflect the uncertainty degree of the system failure. More specifically, our previous work (Saravi et al., 2022) proposed a two-stage resilience-constrained expansion planning model for IDSs, including PDS, GDS, and district heating system (DHS), which introduces a new framework considering a coordinator unit for interaction between IDSs. A decentralized structure for solving the two-stage problem has been introduced using a modified linearized alternating direction method of multipliers with parallel splitting and the adaptive penalty (LADMMPSAP), which results in simplicity and computational efficiency. A novel structure for MCEMs, including power, heat, and hydrogen energy carriers, considering P2G technologies, is proposed in Mansour-Saatloo et al. (2021). A decentralized energy management approach using the alternating direction method of multipliers (ADMM) algorithm is used to decentralize the model and preserve the privacy of MCEMs. Integration of MCEMs could improve overall energy efficiency through cascaded energy usage and enhance system flexibility by incorporating DER (Good & Mancarella, 2019; Krause et al., 2011). DC-MGs have attracted wide attention in recent years since DC systems are free from reactive power, frequency, and synchronization issues with more overall reliability and efficiency (Al-Ismail, 2021; Jithin et al., 2022). Other research (Ahmed et al., 2018; Ouyang et al., 2022; Zhang et al., 2022) has demonstrated the technical and economic benefits of incorporating DC systems in PDSs than in purely AC systems, involving lower power losses, enhanced voltage profile, higher transmission capacity, and lower investment costs. PDS planners need to make decisions about scenarios for the configuration of PDSs and Power MGs (PMGs) in expansion planning (Liu et al., 2022; Qu et al., 2022). These scenarios include developing pure AC-PDSs and AC-PMGs, pure DC-PDS and DC-PMGs, or hybrid AC and DC scenarios. However, research in DC or hybrid AC-DC-PDSs is still in the infant stage and needs a comprehensive investigation and an expansion planning perspective. Most of the existing literature focuses on investigating the operational aspects of IDSs to enhance resilience, while including resilience in the long-term planning problem of IDSs requires further research. Furthermore, previous studies have predominantly examined the planning of IDSs and MCEMs separately, without considering the coordinated planning of IDSs and MCEMs as independent energy agents with energy trading capabilities. More research on coordinated planning is needed to ensure the understanding of the synergistic benefits and potential trade-offs between IDSs and MCEMs. The impacts of expanding DC grids within existing PDS infrastructures on the planning cost and resilience improvement of the IDSs and MCEMs have yet to be investigated in the literature. A tri-level, two-stage, coordinated resilience-oriented stochastic expansion planning model for IDSs and MCEMs is proposed in this paper to address these research gaps. This model aims to fill the aforementioned research gaps by considering the integration of resilience into the expansion planning problem, exploring coordinated expansion planning (CEP) of IDSs and MCEMs, and investigating the effects of incorporating DC grid expansions on the cost minimization and resilience improvement of the system. The IDSs include AC or DC-type PDS, GDS, and DHS, while the MCEMs include AC or DC-type PMG, gas MG (GMG), and heat MG (HMG). The DC-PDS constituting with existing AC-PDS and expansion of AC or DC PMGs are considered as the scenarios in the model to investigate the impacts of these configurations on the planning problem and to clear the impacts of developing DC-PDS and PMGs on the system's resilience. The key contributions of this paper can be listed as follows:

(1) A resilience-oriented model for coordinated expansion planning of IDSs and MCEMs is proposed. This model can be used as a benchmark for assessing collaboration plans between distribution system operators (DSOs) and MG system operators (MGSOs), considering the resilience improvement of the whole system.
(2) The proposed model finds the optimal AC-DC configuration of PDS and PMGs in the planning problem. The existing PDS can be operated by DC power.
(3) A tri-level two-stage stochastic model for coordinated expansion planning of IDSs and MCEMs is developed. The objective function of the first stage is to minimize the investment and operation costs in the planning horizon. The second stage aims to minimize resilience costs imposed in an emergency condition. A proper resilience maximization index (RI) is used at this stage. A linearized convex tractable reformulation for the proposed model is developed. A combined adaptive dynamic programming (ADP) with the LADMMPSAP algorithm is proposed to solve the problem efficiently.
(4) A variation of the aggregator-agent splitting using the agent coupling coordinator (ACC) is introduced. This proposed framework interacts with related agents in IDSs and MCEMs, distributing the computational burden over the agents and preserving agents' privacy. On this basis, LADMMPSAP is employed, which fits more than two blocks of variables and helps faster convergence.

The remainder of the paper is organized as follows: Section 2 introduces the problem description for the planning problem. Section 3 explains the problem formulation and provides a detailed model for couplings of agents. The solution procedures and the planning methodology are outlined in Section 4. Section 5 describes the case study employed for evaluating the effectiveness of the proposed CEP model. The final section presents the conclusions.

2. Problem description

To fill the mentioned gaps in Section 1, a coordinated expansion planning of the IDSs and MCEMs is proposed, as shown in Fig. 1. The ACC unit is introduced as the aggregator to exchange the technical and price information between agents. It is assumed that in scenarios in which the proposed CEP is studied, the expansion of IDSs will be done through MCEMs so that the demand growth during the planning period is taken into account via MGs. MGs are independent agents with a private owner and have independent operators. The main problem is to minimize expansion planning costs for the whole system, including IDSs and MCEMs, in the planning period. In the proposed framework, MGs will send the amount and price for exchange energy via the IDSs to the ACC to maximize their profit. A vital feature in the proposed model is the couplings of energy systems at both IDSs and MCMEs levels. Integrating resilience into the CEP problem of the proposed model is a significant step towards developing more robust and resilient IDSs. By introducing a normalized resilience index (RI), the model considers both the disruption and recovery phases, offering a comprehensive evaluation of resilience in IDSs. Stage 2 of the model focuses on maximizing resilience while minimizing the costs associated with

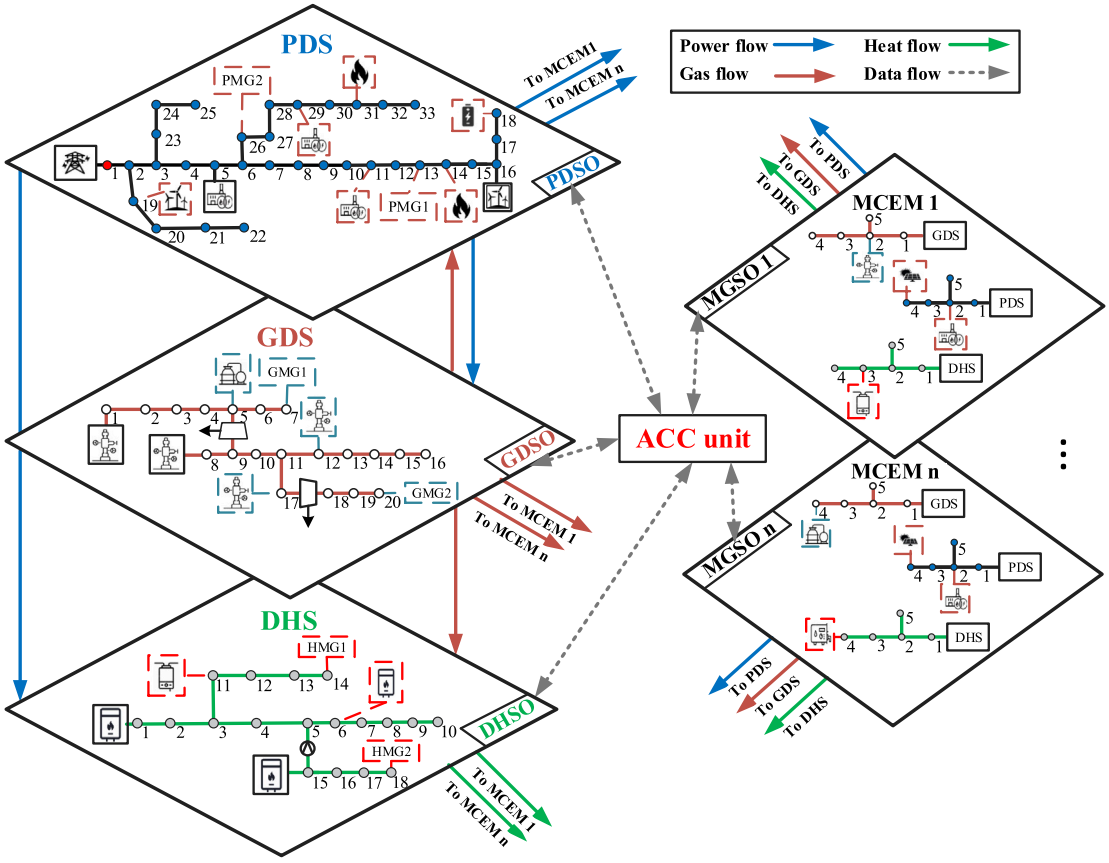

Fig. 1. The proposed IDNs couplings and energy flow.

resilience improvement. This approach acknowledges the importance of considering both the efficacy of recovery measures and the economic aspects of enhancing resilience. By optimizing the proposed RI during emergency conditions, the model identifies optimal recovery measures that contribute to the system's overall resilience. What sets this model apart is the direct impact of the resilience-constrained problem in stage 2 on the CEP cost minimization problem in stage 1. The results obtained from stage 2, including reinforcement scenarios, tie-line installations, and unsupplied demands, are fed into stage 1, where the CEP problem is addressed. This integration ensures that the resilience-focused decision-making in stage 2 directly influences the overall expansion planning process. By incorporating resilience as a constraint within the expansion planning problem, the model accounts for the potential impacts of extreme events, such as hurricanes, on the IDSs. It allows distribution system planners to prioritize reinforcement measures, tie-line installations, and operational strategies that enhance the system's resilience against hurricanes and other disruptive events. This comprehensive approach to integrating resilience into the expansion planning problem ensures that the resulting IDSs and MCEMs are better equipped to withstand and recover from HR events, ultimately improving the overall resilience and performance of the IDSs in the face of disruptions.

3. Formulation and methodology

3.1. PDS and PMG models

Taking into account the possibility of PMG connected to PDS being AC or DC, the model finds the optimal AC-DC hybrid configuration of PDS and PMGs by considering different scenarios of AC and DC combination. The mathematical model of AC and DC networks is presented in the continuation of this section.

3.1.1. AC network model

The AC power flow mathematical model in (1) is established from the linearized model developed in Amirioun et al. (2019) and Saravi et al. (2022).

$$\sum_{g\in\Omega^{g}_{PDS}} P_{i,g,t} + \sum_{i\in\Omega^{Co}_{PDS}} P^{ex}_{i,t} - \sum_{s\in\Omega^{s}_{PDS}} (P^{ch}_{i,s,t} - P^{dis}_{i,s,t}) - P^{D}_{i,t} + P^{DR}_{i,t} = P^{inj}_{i,t} \quad \forall i \in \Omega^{n}_{PDS} \tag{1a}$$

$$\sum_{g\in\Omega^{g}_{PDS}} Q_{i,g,t} + \sum_{i\in\Omega^{Co}_{PDS}} Q^{ex}_{i,t} - Q^{D}_{i,t} + Q^{DR}_{i,t} = Q^{inj}_{i,t} \tag{1b}$$

$$P^{inj}_{i,t} = (2V_{i,t}-1)G^{y}_{ii} + \sum_{\substack{j\in\Omega^{n}_{PDS}\\ j\neq i}} (\theta_{i,t}-\theta_{j,t})B^{y}_{ij} + \sum_{\substack{j\in\Omega^{n}_{PDS}\\ j\neq i}} (V_{i,t}+V_{j,t}-1)G^{y}_{ij} \tag{1c}$$

$$Q^{inj}_{i,t} = -(2V_{i,t}-1)B^{y}_{ii} - \sum_{\substack{j\in\Omega^{n}_{PDS}\\ j\neq i}} (\theta_{i,t}-\theta_{j,t})G^{y}_{ij} - \sum_{\substack{j\in\Omega^{n}_{PDS}\\ j\neq i}} (V_{i,t}+V_{j,t}-1)B^{y}_{ij} \tag{1d}$$

$$\underline{P}_{i,g} \le P_{i,g,t} \le \overline{P}_{i,g} \tag{1e}$$

$$\underline{Q}_{i,g} \le Q_{i,g,t} \le \overline{Q}_{i,g} \tag{1f}$$

$$\underline{V}_{i} \le V_{i,t} \le \overline{V}_{i} \tag{1g}$$

$$0 \le P^{DR}_{i,t} \le P^{Sh}_{i,t} \tag{1h}$$

$$P_{ij,t} = G^{line}_{i,j}(V_{i,t}-V_{j,t}) - B^{line}_{i,j}(\theta_{i,t}-\theta_{j,t}) \tag{1i}$$

$$Q_{ij,t} = -B^{line}_{i,j}(V_{i,t}-V_{j,t}) - G^{line}_{i,j}(\theta_{i,t}-\theta_{j,t}) \tag{1j}$$

$$\underline{S}_{ij} \le S_{ij,t} \le \overline{S}_{ij} \tag{1k}$$

$$(P^{Imp}_{t})^2 + (Q^{Imp}_{t})^2 \le (\overline{S}^{Imp})^2 \tag{1l}$$

$$P_{ij,t} + P_{ji,t} \le \overline{P}_{ij}^{loss} \tag{1m}$$

3.1.2. DC network model

DC-PDS and DC-MGs have been marked by a significant increase in interest for numerous applications due to higher efficiency, better controllability, better integration of renewable energy sources, better compliance with consumer electronics, no issues with reactive power flow and frequency stability, resulting in a notably less complex power system (Dragicevic et al., 2018). The mathematical power flow model for DC-PDS is presented by (2). VSCs can independently control active and reactive power and bidirectional power flow control in AC-DC systems. Thus, the proposed CEP model employs VSCs for AC-DC power conversion. The steady-state model of VSC is expressed in (2h)–(2j) for a VSC connected between AC bus i and DC bus j. According to Ahmed et al. (2018), the relation between AC and DC bus base voltage and per-unit voltage can be described by (2h) and (2i), respectively. The AC and DC active power of VSC are related by (2j) with the converter efficiency, η^{vsc}.

$$\sum_{g\in\Omega^{g}_{PDS}} P_{g,t} + \sum_{i\in\Omega^{Co}_{PDS}} P^{ex}_{i,t} - \sum_{s\in\Omega^{s}_{PDS}} (P^{ch}_{s,t} - P^{dis}_{s,t}) - P^{D}_{i,t} + P^{DR}_{i,t} = P^{inj}_{i,t} \quad \forall i \in \Omega^{n}_{PDS} \tag{2a}$$

$$P^{inj}_{i,t} = \sum_{\substack{j\in\Omega^{n}_{PDS}\\ j\neq i}} P_{ij,t} \tag{2b}$$

$$P_{ij,t} = G^{line}_{i,j} V_{i,t}(V_{i,t} - V_{j,t}) \tag{2c}$$

$$\underline{P}_{i,g} \le P_{i,g,t} \le \overline{P}_{i,g} \tag{2d}$$

$$\underline{V}_{i} \le V_{i,t} \le \overline{V}_{i} \tag{2e}$$

$$\underline{P}_{ij} \le P_{ij,t} \le \overline{P}_{ij} \tag{2f}$$

$$0 \le P^{DR}_{i,t} \le P^{Sh}_{i,t} \tag{2g}$$

$$V^{ac,base}_{i} = K^{vsc} V^{dc,base}_{j} \tag{2h}$$

$$V^{ac,pu}_{i} = M^{vsc} V^{dc,pu}_{j} \tag{2i}$$

$$P^{ac}_{i} = \frac{P^{dc}_{j}}{\eta^{vsc}} \tag{2j}$$

The superscripts ac and dc are used to show the voltage and power value on the VSC's AC and DC sides. The superscripts base and pu (2h) and (2i) show the base and per-unit values of the voltage. The converter constant value, K^{vsc}, for the three-phase VSC with a sinusoidal pulse-width modulation is equal to $(\sqrt{3}/2\sqrt{2})$ (Ahmed et al., 2018). It is assumed that the modulation index of VSC M^{vsc} is equal to 1 in all cases studied. The presented model is a non-linear which can be converted into a linearized equivalent with the help of alternative variables $u_i = V_i^2$ and $W_{ij} = V_i V_j$. The piecewise linearization method, as done in Liu et al. (2019), is used to linearize the term $V_i V_j$. Therefore, Eqs. (2c) and (2e) are substituted with (3a) and (3b), respectively.

$$P_{ij,t} = G^{line}_{i,j}(u_{i,t} - W_{ij,t}) \tag{3a}$$

$$\underline{V}_{i}^{2} \le u_{i,t} \le \overline{V}_{i}^{2} \tag{3b}$$

The mathematical models of AC and DC power flow for PMGs are similar to (1) and (2) unless the sets in the PDS should be replaced with the corresponding ones for the PMGs, i.e. Ω^{g}_{PMG}, Ω^{Co}_{PMG}, Ω^{s}_{PMG}, Ω^{n}_{PMG}.

3.2. GDS and GMG models

The GDS and GMG consist of town board stations (TBSs) as gas sources, pipelines, natural gas storage (GS), gas compressors (GCs), and demand. The steady-state gas flow model in (4) is established based on (Huang et al., 2019). The mass balance in nodes and gas flow in pipelines are expressed in (4b) and (4c), respectively. The gas flow in pipelines is restricted by (4c). Constraint (4d) confirms an acceptable gas production of gas sources. The gas exchange between GDS and GMGs will be limited by the coupling pipeline's gas flow limitation expressed in (4c). The DR can be applied to the non-critical demands in the introduced bounds in (4e). The active pipelines are compensated by GC, which puts the gas pressure of pipelines in the bounds given in (4f).

$$\sum_{g\in\Omega^{g}_{GDS}} q_{k,g,t} + \sum_{k\in\Omega^{Co}_{GDS}} q^{ex}_{k,t} - \sum_{s\in\Omega^{s}_{GDS}} (q^{ch}_{k,s,t} - q^{dis}_{k,s,t}) - q^{D}_{k,t} + q^{DR}_{k,t} = \sum_{\substack{l\in\Omega^{n}_{GDS}\\ k\neq l}} q_{kl,t} \tag{4a}$$

$$q^{2}_{kl,t} = sign(q_{kl,t})\psi^{2}_{kl}(\Gamma_{k,t} - \Gamma_{l,t}) \tag{4b}$$

$$\underline{q}_{kl} \le q_{kl,t} \le \overline{q}_{kl} \tag{4c}$$

$$\underline{q}_{k,g} \le q_{k,g,t} \le \overline{q}_{k,g} \tag{4d}$$

$$0 \le q^{DR}_{k,t} \le \overline{q}^{Sh}_{k,t} \tag{4e}$$

$$\Gamma_{k,t} \le \Gamma_{l,t} \le \zeta_{kl}\Gamma_{k,t} \tag{4f}$$

A piecewise linearization method, as done in Li et al. (2017), is employed to have a linear model and reduce the complexity of the model.

3.3. DHS and HMG models

A steady-state thermal-hydraulic model is used to model the DHS and HMGs. The nodal mass balance and water flow of DHS in steady-state are expressed in (5a) and (5b), respectively. The nonlinear "Weymouth equation" in (5b) is linearized by the linearization method used for (4b). The heat loss along the pipelines is computed by (5c), and the nodal temperature of the mixed water is calculated using (5d) according to Saravi et al. (2022). Eq. (5e) states that the temperature of mass flowing out of the pipeline mr is equal to the mixed temperature at the start node r. The upper and lower bounds of mass flow in heat sources and pipelines are expressed in (5f) and (5g), which limits the heat exchange using coupled pipelines between DHS and HMGs. The node's water pressure and temperature are constrained by (5i) and (5j).

$$\sum_{g\in\Omega^{g}_{DHS}} M_{m,g,t} + \sum_{m\in\Omega^{Co}_{DHS}} M^{ex}_{m,t} - \sum_{s\in\Omega^{s}_{H}} (M^{ch}_{m,s,t} - M^{dis}_{m,s,t}) - M^{D}_{m,t} + M^{DR}_{m,t} = \sum_{\substack{r\in\Omega^{n}_{DHS}\\ m\neq r}} c^{w} m_{mr,t}(\tau^{in}_{mr,t} - \tau^{out}_{mr,t}) \tag{5a}$$

$$m^{2}_{mr,t} = sign(m_{mr,t})\psi^{2}_{mr}(\Pi_{m,t} - \Pi_{r,t}) \tag{5b}$$

$$(\tau^{out}_{mr,t} - \tau^{a}) = (\tau^{in}_{mr,t} - \tau^{a})\varphi_{mr} \tag{5c}$$

$$\tau^{mix}_{r,t} \sum_{mr\in\Omega^{L}_{DHS}} m_{mr,t} = \sum_{mr\in\Omega^{L}_{DHS}} m_{mr,t}\tau^{out}_{mr,t} \tag{5d}$$

$$\tau^{in}_{mr,t} = \tau^{mix}_{r,t} \quad \forall mr \in \Omega^{L}_{DHS} \tag{5e}$$

$$\underline{m}_{m,g} \le m_{m,g,t} \le \overline{m}_{m,g} \tag{5f}$$

$$\underline{m}_{mr} \le m_{mr,t} \le \overline{m}_{mr} \tag{5g}$$

$$\underline{\Pi}_{m} \le \Pi_{m,t} \le \overline{\Pi}_{m} \tag{5h}$$

$$\underline{\tau}_{m} \le \tau_{m,t} \le \overline{\tau}_{m} \tag{5i}$$

$$0 \le M^{DR}_{m,t} \le \overline{M}^{Sh}_{m,t} \tag{5j}$$

The maximum load curtailment using the DRP for non-critical loads is expressed in (5j).

3.4. Energy storage system (ESS) model

The ESSs include battery energy storage system (BESS), GS, and thermal storage (TS). The mathematical formulation of ESSs is stated

in (6), which is taken from Saravi et al. (2022). A common symbol y is used to shorten the text, which stands for P, q, and M in power, gas, and heat energy agents, respectively.

$$SoC_{N,s,t} = SoC_{N,s,t-1} + \frac{\eta^{ch}_{N,s} y^{ch}_{N,s,t} \Delta t}{\overline{E}_{N,s}} - \frac{y^{dis}_{N,s,t} \Delta t}{\eta^{dis}_{N,s} \overline{E}_{N,s}} \tag{6a}$$

$$\underline{SoC}_{N,s} \le SoC_{N,s,t} \le \overline{SoC}_{N,s} \tag{6b}$$

$$0 \le y^{ch}_{N,s,t} \le \overline{y}^{ch}_{N,s} x^{ch}_{N,s,t} \tag{6c}$$

$$0 \le y^{dis}_{N,s,t} \le \eta^{dis}_{N,s} \overline{y}^{dis}_{N,s} (1 - x^{ch}_{N,s,t}) \tag{6d}$$

3.5. Integrated model

The coupling components that integrate IDSs and MCEMs are CHP, P2G, GB, electric boiler (EB), GC, and water pump (WP) in this paper. The multi-energy efficiency matrix K with the 4×5 dimension denotes the couplings of IDSs and MCEMs. The model of coupling components is incorporated in the multi-vector flow in (7a), which couples the distributed energy systems with each other. The terms on the right side of (7a) show the generation of related buses and nodes of the coupled agent. In the multi-energy efficiency matrix, there are as many rows as consumed energy in conversion components energy and as many columns as generated energy from conversion components. For example, two columns exist for power and heat generation from CHP and one row for gas consumption in CHP. The CHPs and P2Gs are installed in PDS and PMGs, while EBs and GBs are installed in DHS and HMGs. Therefore, $\hat{\imath}$, $\hat{k}$ and, $\hat{m}$ are used to express the bus or nodes in which the conversion components consume energy and also the DHS and the HMG which the CHPs heat generation is injected. Elements k_1 to k_6 of the matrix are the relevant conversion efficiency from one energy vector to another one which details of their calculations can be found in Li et al. (2016), Liu and Mancarella (2016) and Saravi et al. (2022). The GC and WP are two other conversion components in the model, which have different models. The GC reduces the gas volume to increase the pressure of a gas by power consumption. The compression power consumption can be calculated using (7b), which is related to the ratio of output and input pressure in nodes k and l and the mass flow through the compressor (Saravi et al., 2022). The passing mass flow and the pressure ratio between the input and output of the compressor are limited by (7c) and (7d), respectively. WPs are used to overcome the distribution pressure losses along the DHSs. The pumping power is calculated using (7e) based on Li et al. (2016), which is related to the flow rate passing by the pump and the pressure difference between the input and output points of the pumps.

$$\begin{pmatrix} q^{D,CHP}_{\hat{k},t} \\ q^{D,GB}_{\hat{k},t} \\ P^{D,EB}_{\hat{\imath},t} \\ P^{D,P2G}_{\hat{\imath},t} \end{pmatrix} = \overbrace{\begin{pmatrix} k_1 & k_2 & 0 & 0 & 0 \\ 0 & 0 & k_3 & 0 & 0 \\ 0 & 0 & 0 & k_4 & 0 \\ 0 & 0 & 0 & 0 & k_5 \end{pmatrix}}^{K} \begin{pmatrix} P_{i,g} \\ M_{\hat{m},g} \\ M_{m,g} \\ M_{m,g} \\ q_{\hat{k},g} \end{pmatrix} \tag{7a}$$

$$P^{D,GC}_{\hat{\imath},t} = k_6 q_{kl,t} \left(\left(\frac{\Gamma_{l,t}}{\Gamma_{k,t}}\right)^{k_7} - 1 \right) \tag{7b}$$

$$\underline{q}_k \le q_{k,t} \le \overline{q}_k \tag{7c}$$

$$\underline{CR} \le \left(\frac{\Gamma_{l,t}}{\Gamma_{k,t}}\right) \le \overline{CR} \tag{7d}$$

$$P^{D,WP}_{\hat{\imath},t} = k_8 m_{mr,t} (\Pi_{m,t} - \Pi_{r,t}) \tag{7e}$$

In the case of the GC and WP, it is assumed that they have the same flow and pressure input and output values as the nodes they are connected to.

4. CEP model

The tri-level stochastic CEP framework for IDSs and MCEMs that considers resilience and MCEMs energy trading with IDSs is shown in Fig. 2. The optimization model is a MILP with many coupling variables between IDSs and MCEMs using the ACC unit. The proposed tri-level model is established in this section. The stochastic expansion planning model of IDSs and MCEMs is formulated on the first level to minimize the total investment and operation costs while satisfying the operational constraints of IDSs and MCEMs. For the PDS and PMGs, the AC or DC configuration is considered using scenarios impacting investment, operation, and resilience costs. On the second level, given the expansion planning of agents, the objective is to maximize the profit of MCEMs by exchanging energy with the IDSs. A resilience cost minimization objective in emergency conditions constrained to RI maximization forms the third level. As the master problem, the first level sends the planning scenarios and variables to the second level. The second level provides feedback on the MCEM's energy exchange and price bids to the master problem. In emergency conditions, the third level runs to maximize the system's resilience by implementing MG (Microgrid) formation, DRP, load shedding, and line reinforcement. The respective discussion on objective functions, decision variables, and constraints is presented in the continuation of this section. These factors influence the energy exchanges at the second level and consequently impact the planning costs of the first level.

4.1. Firs level problem

On the first level, the stochastic CEP model is developed to minimize the investment and operation costs' net present value (NPV) while satisfying the capacity requirements of IDSs and MCEMs. The first level model is formulated as follows:

$$C^{CEP} = \min \sum_{\xi} \Theta_{\xi} (r^{\frac{P}{A}}_{\xi,T} C^{Inv} + r^{\frac{P}{F}}_{\xi,y} C^{Op}) \tag{8a}$$

$$C^{Inv} = \sum_{N \in \Omega_N} \sum_{y \in Y} \left(r^{\frac{A}{P}}_{\xi,T_L} \sum_{L \in \Omega^L_N} (x_{N,L,y} IC_{N,L} + x^{(r)}_{L,y} IC^{(r)}_L) \right.$$
$$\left. * + r^{\frac{A}{P}}_{\xi,T_g} \sum_{g \in \Omega^{g,(n)}_N} x_{N,g,y} IC_{N,g} + r^{\frac{A}{P}}_{\xi,T_s} \sum_{s \in \Omega^{s,(n)}_N} x_{N,s,y} IC_{N,s} \right) \tag{8b}$$

$$C^{Op} = \sum_{N \in \Omega_N} \sum_{y \in Y} (OC^F + OC^V) \tag{8c}$$

$$OC^F = \sum_{L \in \Omega^L_N} OC^F_{N,L,y} + \sum_{g \in \Omega^g_N} OC^F_{N,g,y} + \sum_{s \in \Omega^s_N} OC^F_{N,s,y} \tag{8d}$$

$$OC^V = \sum_{\mathbb{S} \in \Omega_{\mathbb{S}}} N_{\mathbb{S}} \sum_{t \in T_d} \left(\sum_{g \in \Omega^g_N \cup \Omega^{slack}_N} E_{N,g,y,\mathbb{S},t} C^{RTP}_{N,y,\mathbb{S},t} + P^{loss}_{N,y,\mathbb{S},t} C^{loss} \right) \tag{8e}$$

$$\sum_{L \in \Omega^L_N} (x_{N,L,y} IC_{N,L} + x^{(r)}_{L,y} IC^{(r)}_L) + \sum_{g \in \Omega^{g,(n)}_N} x_{N,g,y} IC_{N,g}$$
$$+ \sum_{s \in \Omega^{s,(n)}_N} x_{N,s,y} IC_{N,s} +$$
$$* OC^F + OC^V + (E^P_{N,y,\mathbb{S},t} \Pi^P_{N,y,\mathbb{S},t} - E^S_{N,y,\mathbb{S},t} \Pi^S_{N,y,\mathbb{S},t}) \le C^{Budget} \tag{8f}$$

$$Cons(1)\text{–}(5) \tag{8g}$$

Where the terms $r^{\frac{P}{A}}_{\xi,T}$, $r^{\frac{A}{P}}_{\xi,T}$, $r^{\frac{P}{F}}_{\xi,T}$ are time value of money that converts a present value to its equivalent annual value, an annual value to its equivalent present value, and a future value to its equivalent present value with interest rate $r_{\xi,T}$ over time T, respectively, which the details of calculation can be found in Khaligh and Anvari-Moghaddam (2019). In this model, (8a) expresses the CEP costs, including investment and operation. Eqs. (8b) and (8c) show the details of investment and

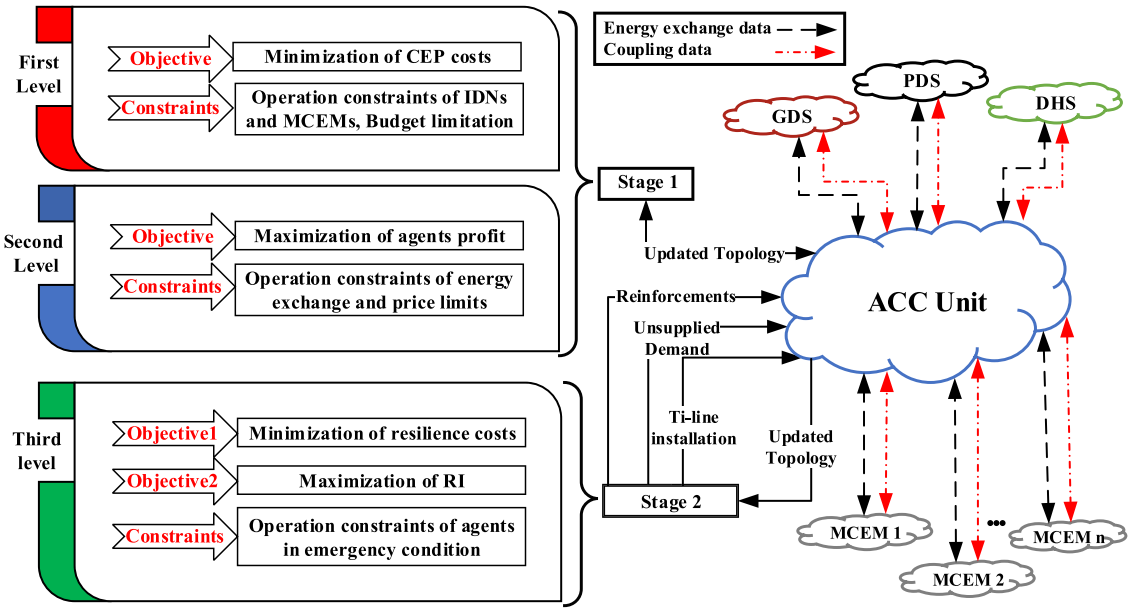

Fig. 2. The proposed framework for CEP.

operation costs in the model, respectively. Investment costs of new generation units, storage units, and new lines are considered; the reinforcement of existing lines is also added in (8b). According to (8c), operation costs consist of fixed and variable costs, which are expressed in (8d) and (8e), respectively. A common symbol E is used in (8e) to shorten the text, which stands for P, q, and M in power, gas, and heat energy agents respectively. The first term in (8e) represents purchasing energy from the upstream grid or generation units from other distribution systems and MGs with the real-time price of that agent and, for example, purchasing heat energy of CHP units in DHSs from PDS. The second term expresses the cost of power loss. To incorporate a more realistic model, the constraint of the annual budget limit is considered as (8f). The operational limitations are outlined in (8g).

4.2. Second level problem

At the second level, MCEMs desire to maximize their energy exchange profit and thus reduce their network expansion costs. For this purpose, according to the capacity and the price signals sent by the MGSOs to the ACC unit, they determine their desired amount and price of exchange energy. The mathematical model of the second level is developed as follows:

$$C^{Pr} = \max \sum_{\xi} \Theta_{\xi} \sum_{N\in\Omega_N} \sum_{y\in Y} \sum_{\mathbb{S}\in\Omega_{\mathbb{S}}} \sum_{t\in T_d} (E^{S}_{N,y,\mathbb{S},t} \Pi^{S}_{N,y,\mathbb{S},t} - E^{P}_{N,y,\mathbb{S},t} \Pi^{P}_{N,y,\mathbb{S},t}) \tag{9a}$$

$$0 \le \Pi^{S}_{N,y,\mathbb{S},t} \le \overline{\Pi}^{S}_{N} \tag{9b}$$

$$0 \le \Pi^{P}_{N,y,\mathbb{S},t} \le \overline{\Pi}^{P}_{N} \tag{9c}$$

$$Cons(1a), (4c), (5g) \tag{9d}$$

The profit of MCEMs expressed in (9a) consists of two terms; the first term shows the income from selling energy to IDSs, while the second term represents the cost of energy purchased from the IDSs. The energy selling and purchasing prices for MCEMs are limited by (9b) and (9c), respectively. It should be noted that the maximum energy exchange between MCEMs and IDSs is restricted by limitations of the coupling lines, as indicated in (1k), (2f), (4c), and (5g).

4.3. Third level problem

The third level involves two objective functions: resilience cost minimization and RI maximization for the whole system. This multi-objective optimization problem is converted into a single objective problem using the min–max regret method inspired by Moreira et al. (2018). This level is defined in the emergency condition time interval, $T_e = [t_d, t_r]$, which is due to the hurricane occurrence. The resilience cost objective shown in (10a)–(10c) comprises three terms: unsupplied energy in the IDSs and MCEMs arising from failure in the PDS, financial losses, C_N^{repair}, due to poles and conductor failure in the PDS and PMGs, and the value of lost load (VoLL) for customers. It is assumed that the unsupplied energy cost $C^{DR}_{N,y,\mathbb{S},t}$ is equal to the maximum price of energy in the understudy day at that agent. A pessimistic condition assumes that the hurricane incident will occur from 16:00 to 21:00, the peak load time. The repairing time for the damaged lines is assumed to be constant and equal to three hours. The recovery measurements for the resilience improvement are the line reinforcement in the PDSs and PMGs, MG formation in IDSs considering MCEMs, and load shedding. The RI maximization as the second objective is defined using a normalized RI in (10d), which is a proper dynamic index for studying resilience improvement from the planning perspective since it considers the whole resilience range, including disruption and recovery phases. ν is a set of wind profile speed scenarios according to the Saffir-Simpson category. The hurricane wind speed model (a spatially-time varying called the Holland model) and failure probability of overhead lines in PDS and PMGs under the hurricane is considered according to Saravi et al. (2022). Wind turbines are especially vulnerable to hurricanes as the maximum wind speeds can exceed their cut-off limits. Therefore, modeling wind turbine tripping during hurricanes can be achieved using probabilistic methods, as described in Adnan et al. (2021). However, adopting a risk-averse approach, wind turbines are assumed to shut down during hurricanes. On the other hand, for overhead lines, the probability of failure is calculated using fragility curves specific to poles and conductors. The GDS and DHS pipelines are located underground, so they are safe in a hurricane. Reinforcement of power lines means replacing poles with poles of a higher class for classes 3 and 4 and replacement with new poles of the same class for poles of class 2. The candidate lines in PDS and PMGs for reinforcement are determined by (10e).

$$C^{Re} = \min \sum_{\nu} \Theta_{\nu} r^{\frac{P}{F}}_{\xi,y} C^{RI}_{\xi,\nu} \tag{10a}$$

$$C^{RI}_{\xi,\nu} = \sum_{N\in\Omega_N}\sum_{y\in Y}\sum_{\mathbb{S}\in\Omega_{\mathbb{S}}}\sum_{t\in T_e}\left(E^{DR}_{N,y,\mathbb{S},t}C^{DR}_{N,y,\mathbb{S},t} + C^{repair}_{N,y,\mathbb{S}} + E^{DR}_{N,y,\mathbb{S},t}C^{LL}_{N}\right) \quad (10b)$$

$$C^{repair}_{N,y,\mathbb{S}} = N^{FP}C^{rep}_{pole} + L^{FC}C^{rep}_{con} \quad (10c)$$

$$RI_t = \max \sum_{t_d}^{t_r}\omega_N \frac{E_{N,t_d} - E^{DR}_{N,t_d}}{E_{N,t_d}(t_r - t_d)} \quad (10d)$$

$$\Omega^f_N = \{L|P^f_L \rangle P^f_{Th}\}\ ,\ t\in T_e\ ,\ N\in\{PDS, PMGs\} \quad (10e)$$

$$Cons(1)\text{–}(5) \quad (10f)$$

As mentioned earlier, E stands for P, q, and M in power, gas, and heat energy networks, respectively. The operational constraints are expressed in (10f). After a hurricane, the PDS forms islands, considering the PMGs to supply the disrupted demands from the upstream grid. Therefore, new constraints must be considered to ensure the radiality of the PDS. Thus, the operational constraints of the PDS in (10f) are reformulated to account for the islands formed after hurricanes, using the proposed method in Arif et al. (2018). To convert the multi-objective optimization problem into a single objective problem at the third level, a modified min–max regret method, as described in Moreira et al. (2018), is introduced in (11). By applying the modification to (11), the model is developed for a two-level optimization using normalized objective functions.

$$\min_{z\in Z} Reg(z) \quad (11a)$$

$$Reg(z) = \max_{s\in S,\hat{x}\in X}(\hat{\Psi}_1(z,\hat{x},s) - \hat{\Psi}_2(z,\hat{x},s) - \hat{\Psi}^{\star}_{\hat{x},s}) \quad (11b)$$

$$Cons(10f) \quad (11c)$$

Where $\Psi_1(.)$ and $\Psi_2(.)$ are the objective functions corresponding to the functions expressed in (10a) and (10d), respectively. X and Z are the feasible set of solutions in the first and second stages of the CEP problem. S is the set of all defined strategies in the second stage problem, including line reinforcement, MG formation, and load shedding. $\hat{x}$, z are the solution vector in the first and second stage, respectively, and s is the vector of the strategies scenario. $\hat{\Psi}^{\star}_{\hat{x},s}$ is the optimal value of $\hat{\Psi}_1(z^{\star},\hat{x},s) - \hat{\Psi}_2(z^{\star},\hat{x},s)$ by optimal solution $z^{\star}$ under scenario s. The normalized objective functions $\hat{\Psi}_1(.)$ and $\hat{\Psi}_2(.)$ using ideal and nadir point based on the straightforward objective normalization method represented in He et al. (2021).

4.4. Solution methodology

Adopting an appropriate model for solving the optimization problem is a prerequisite for making benefits of CEP of the IDSs and MCEMs. Since IDSs and MCEMs have a separate owner and operator, a multi-agent problem as an assembly of MILP problems communed through coupling components is considered. Each agent solves a MILP problem and has a stake in the master problem. To cope with the computational complexity of a large-scale centralized CEP problem, an aggregator-agent splitting model of LADMMSAP is introduced. This model results in a distributed ADMM formulation, where a central computation unit, called ACC, plays the aggregator role. In contrast to a centralized solution, the ACC primarily focuses on exchanging information between agents and performing computationally simple tasks. The majority of the computational effort is delegated to be carried out individually by the agents. The CEP problem of (8)–(10) is decomposed with the aggregator-agent LADMMPSAP as follows:

$$f(x_1,x_2,z) = \min \sum_{\xi}\Theta_{\xi}(c^T_1x_1 + c^T_2x_2 + \sum_{\nu}\Theta_{\nu}c^T_3z) \quad x_1\in X_1, x_2\in X_2, z\in Z \quad (12a)$$

$$G(x_1,x_2,z)\le 0, \quad H(x_1,x_2,z) = 0 \quad (12b)$$

Where vector x_1 and x_2 represent the first-stage decision variables, i.e., installation of new capacities and amount and price of exchanged energy between agents, respectively. Vector ξ denotes the uncertainty parameter in the first stage model, including the output power generation of wind farms and PVs, load growth (LG), and interest rate (IR). Second-stage decision variables are denoted by z, including curtailed load, demand reduction by DRP, lines to be reinforced, and MG formation in the PDS in an emergency condition. X_1 and X_2 are feasible sets of first-stage decisions that are related to the first-level and second-level problems, respectively. Z is the feasible set for the second-stage decisions. The terms $c^T_1x_1$ and $c^T_2x_2$ in the objective function corresponds to the investment and operation cost minimization in (8a) and profit maximization in (9a) which is converted to minimization using the negative sign. The term c^T_3z is the resilience cost under uncertainty parameter ν and a given x_1 and x_2 corresponds to the second stage problem in (12). Constraints include those expressed in (1)–(8). The proposed problem is a large-scale multi-time period planning problem that is computationally complex and time-consuming. The search can be significantly reduced by prioritizing likely feasible investment scenarios on the planning horizon. ADP makes a trade-off between optimal and computational time and offers powerful mathematical tools to handle the curse of dimensionality (Xu, Ding, et al., 2020). The search can be significantly reduced by prioritizing feasible scenarios of the problem. The ADP model, according to Xu, Ding, et al. (2020) and Yuan et al. (2022), is used to reduce the search space for the CEP problem. The dynamics of each agent are described by (13a). The action during the ℓth state in the planning horizon takes the form $\hat{A}_{\ell}$ which is a function of the scenario ξ and post-decision state $A^{\alpha}_{\ell} = \Delta_{\ell}\alpha_{\ell}$. At each state, a feasible action α_{ℓ} should be selected. For shorthand, the feasible set is denoted by $\chi_{\ell}(A_{\ell})$, this is the set of action α_{ℓ} that satisfy (13a). Let Π be the family of decision functions that could be chosen, Φ^{π}_{ℓ} maps each state to a feasible action according to (12b). The objective is to select a priority list of feasible scenarios that minimize expected contribution over the planning horizon, as expressed in (13c). In (13d), the simplified power and mass balance considering generation and demand are considered.

$$A_{\ell+1} = \Delta_{\ell}x_{\ell} + \hat{A}^{x}_{\ell} \quad (13a)$$

$$x_{\ell} = \Phi^{\pi}_{\ell} \in \chi(A_{\ell}) \quad (13b)$$

$$\min_{\pi\in\Pi}\mathbb{E}[\sum_{\ell}C_{\ell}X^{\pi}_{\ell}(A_{\ell})] \quad (13c)$$

$$Cons(1a), (2a), (4a) \quad and \quad (8f) \quad (13d)$$

Basic procedures are summarized in Algorithm 1. The LADMMPSAP method is inherited from Saravi et al. (2022). Inspired by this work, the Lagrangian multipliers δ, adaptive penalty factor μ, penalty factor λ, and termination thresholds ϵ calculations are presented in Algorithm 1. A general vector variable y is used to represent the variables that exchange data between agents and the ACC. In each agent sub-problem solving process, $y^{(\kappa+1)}$ is variable while y^{κ} is supposed to be a constant determined by the consensus of the ACC and the coupled agent operator.

5. Case studies and simulations

In order to represent the application and effectiveness of the proposed resilience-oriented CEP model, several case studies are defined for the integrated IDSs and MCEMs shown in Fig. 3. The IDSs consist of the modified, well-known IEEE 33-bus radial PDS coupled with a 20-node GDN and a 16-node DHN. The rated capacities for CHPs, PV farms, wind turbines (WTs), P2Gs, and BESSs in the PDS are the sets of $\{0.5, 0.8, 1, 1.2, 1.5\}$, $\{0.6, 0.8, 1, 1.2\}$, $\{0.6, 0.8, 1, 1.2\}$, $\{0.4, 0.6, 0.8, 1\}$, $\{0.4, 0.6, 0.8, 1\}$ all in MW, respectively. The generation and storage units in the PMGs are considered with rated capacities of 0.2–1 MW with a step size of 0.2 MW. The candidate generation and storage units in the DHN are considered with rated capacities of 0.2–1.6 MW with a step size of 0.2 MW. The PMGs can be either AC or DC based on the requirements to minimize the objective function. In other words,

Table 1
Parameters of candidate components in the PDS and DHS (Saravi et al., 2022).

Component	IC (M$/MW)	Fixed OC ($10^3$$/MW year)	Lifetime (year)
CHP	0.95	19.8	25
WT	1.2	25	20
PV	1.5	18	25
P2G	1.15	50	20
BESS	1.22	15	15
VSC	0.12	6.5	20
EB	0.20	4	20
GB	0.18	12	30
TS	0.12	10	35

the optimization results guide the planners of the PDS and PMGs in deciding whether to develop AC or DC systems. Voltage source converters (VSCs) are utilized for AC-DC power conversion. For the first-level problem, a reconfiguration scenario is defined, involving the installation of line 33 between buses 22 and 26 and the opening of switches on line 25 between buses 6 and 26. The geographical coordination of PDS buses, line and pipeline data of IDSs, and interconnected lines and pipelines can be found in Saravi et al. (2022). The pole classes of the PDS, PMGs line data, couplings between IDSs and MCEMs, and simulation parameters are provided in Appendix.

Algorithm 1 The ADP-LADMMPSAP method

1. Forming feasible scenarios, X_y^{π}, using ADP in (12).
2. Set initial value for $\varepsilon_1, \varepsilon_2, \varepsilon_3 > 0$, $\rho_0 > 1$, $\mu_{max} \gg 1 \gg \mu_0 > 0$.
3. Solving agents individual expansion planning in (11) for scenarios of step 1 and send coupling variables y_{ik} to ACC.
4. Aggregator step- parallel updating of y_{ik}:

$$y_{ik}^{(\kappa+1)} = \delta^{(\kappa)}(y_{ik} - y_{ik'}^{(\kappa)}) + \frac{\lambda^{(\kappa)}}{2}\|(y_{ik} - y_{ik}^{(\kappa)}) + (\frac{y_{ik}^{(\kappa)} - y_{ik'}^{(\kappa)}}{\lambda^{(\kappa)}})\|^2$$

5. Updating $\lambda^{(\kappa)}$ and $\delta^{(\kappa)}$ as following:

$$\delta^{(\kappa+1)} = \delta^{(\kappa)} + \mu^{(\kappa)}(y_{ik}^{(\kappa+1)} - y_{ik'}^{(\kappa)})$$
$$\lambda^{(\kappa)} = \sigma_{ik}\mu^{(\kappa)}$$
$$\mu^{(\kappa+1)} = \min(\mu_{max}, \rho\mu^{(\kappa)})$$
$$\rho = \begin{cases} \rho_0 & \text{if } \mu^{(\kappa)} max(\sqrt{\sigma_{ik}}\|y_{ik}^{(\kappa+1)} - y_{ik}^{(\kappa)}\| < \varepsilon_2 \\ 1 & \text{otherwise} \end{cases}$$

6.Check the stop criteria as follows:
Error 1: $max(\sqrt{\sigma_{ik}}\|y_{ik}^{(\kappa+1)} - y_{ik}^{(\kappa)}\|) < \varepsilon_1$
Error 2: $(\|f(x_1, x_2, z)^{(\kappa+1)} - f(x_1, x_2, z)^{(\kappa)}\|) < \varepsilon_3$
7. Once satisfied, the iteration ends and output the results, otherwise go to step 2.

The Demand profiles of IDSs and MCEMs for the first year of the study are shown in Fig. 4, where the GDN demand in cubic meters per hour is displayed in the second vertical axis on the right side of the diagram. The real-time prices of energy purchasing from the upstream grid and price cap for energy price bidding by MGs to IDSs are illustrated in Fig. 5. As described in Saravi et al. (2022), a seasonal coefficient is utilized to incorporate the effects of seasonal demand variation. This coefficient multiplies the peak demand profile in each season, allowing for the adaptation of the demand profile.

The parameters for the candidate components in the IDSs and MCEMs are listed in the Tables 1–4. The costs associated with BESS include both DC/DC and AC/DC converter costs. In the DC-PDS and DC-PMGs scenarios, the cost of the AC/DC converter will be subtracted from the overall BESS costs. Additionally, the costs of VSC will be added to the costs of the CHP sources.

The total budget limit of the IDSs is $ 3.5 million per year, of which $ 2 million, $ 1 million, and $ 0.5 million per year, respectively, are allocated to PDS, GDS, and DHS. The total budget limit of the MCEMs is $ 1.2 million per year, of which $ 0.5 million, $ 0.4 million, and $ 0.3 million per year, respectively, are allocated to PMGs,

Table 2
Parameters of candidate components in the GDS (Saravi et al., 2022).

Component	IC (M$/m^3)	Fixed OC ($10^3$$/m^3 year)	Lifetime (year)
TBS	0.40	12	20
GS	0.35	8	20

Table 3
Parameters of distribution lines (Saravi et al., 2022).

Component	IC (M$/km)	Fixed OC ($10^3$$/km year)	Lifetime (year)
Power line	0.15	1	40
Pipeline	0.16	1.5	40

Table 4
Parameters of PDN's conductor and accessories.

Component	Cost ($/km)	Impedance (Ω/km)	Max current (Amp)
Conductor 1 (ACSR otter)	770	0.343+j0.328	270
Conductor 2 (ACSR Waxwing)	1000	0.215+j0.296	445
Other	3850	–	–

Table 5
Uncertainty scenarios (Saravi et al., 2022).

Sce.	Prob.	Wind (%)	PV (%)	IR (%)	LG (%)
1	0.28	50	100	5	3
2	0.23	75	75	10	5
3	0.41	50	50	5	4
4	0.08	100	50	15	6

GMGs, and HMGs. DRPs apply to curtail strategies with a maximum of 10% of the hourly demands in IDSs and MCEMs. DSOs are the IDS's asset owner and system operator, while MGOs act as both roles in MCEMs. The existing AC-PDS and various configurations for DC-PDS are illustrated in Fig. 6 based on the introduced configurations for DC-PDS in Zhang et al. (2019). The symmetrical configuration uses only two of the three wires for power transfer, while the third wire is neutral. This configuration has the advantage of low wire utilization. However, suppose a symmetrical configuration without a neutral wire is chosen. In that case, an additional conductor with the same rating can fully utilize the third wire and further increase transfer capacities. In this configuration, the positive and negative poles are formed using two wires. This configuration enhances wire utilization but introduces ground return for handling unbalanced load currents. It is important to note that this ground return approach may have potential safety risks. An asymmetrical configuration with an extra conductor as a neutral wire is chosen for the VSC to convert an existing AC line to DC in this paper. In this configuration, the neutral wire can be loaded with a full rate for the load current with near zero volt potential, reducing insulation costs over this configuration without a neutral wire. Using this configuration, the maximum power capacity of AC lines can increase by 1.587 times. The AC peak voltage is chosen as the DC-PDS operating voltage with a conservative approach. The DC resistance of conductors is determined to be 0.98 times AC resistance, according to Zhang et al. (2019). In certain urban areas with limited space, constructing new power lines becomes impractical. DC-PDS offers advantages, such as increased line capacity, load supply, and integration of distributed generation. The necessity of building new lines can be deferred or eliminated by converting existing AC-PDS to DC-PDS (Zhang et al., 2019). The adoption of DC-PDS enhances the voltage profile and reduces power losses compared to AC-PDS. The improved voltage profile improves power quality and reliability within the distribution network. The reduced power losses result in increased

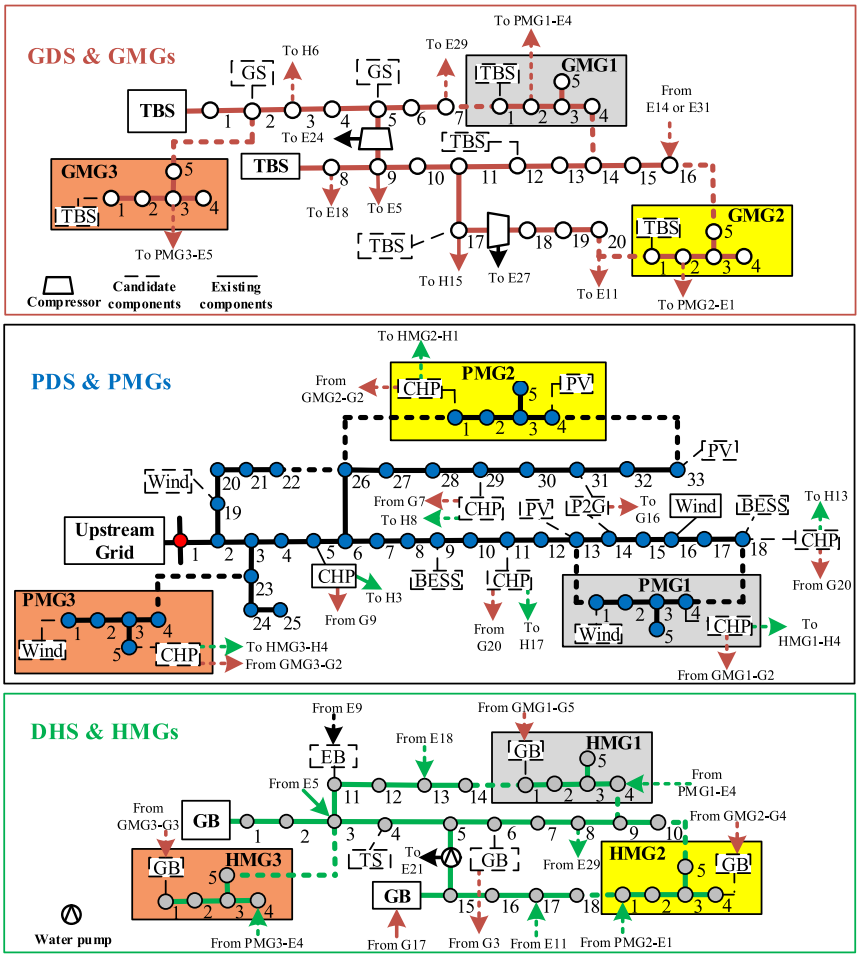

Fig. 3. Integrated IDSs and MCEMs schematic.

energy efficiency and cost savings. While there may be a drawback regarding the cost of building VSCs for the AC to DC conversion, these costs are lower than the expense of constructing new power lines.

The uncertainty scenarios with the associated probabilities of each scenario shown in Table 5 are extracted from Saravi et al. (2022). The details of wind and solar power generation profiles within the understudied area (Florida state in the USA) and data of LG and IR for scenario generation and the process of scenario reduction can be found in Saravi et al. (2022). Detailed information on parameters related to the candidate components, PDS's poles specification, fragility curves of poles with different ages, and hurricane wind speed profiles can be found in Saravi et al. (2022). At the beginning of the planning horizon, an age-dependent fragility curve for poles is utilized based on (Saravi et al., 2022) with the classes 2, 3, and 4 southern pine poles 60 and 30 years old. The hurricane frequency occurrence is specified using a Poisson probability distribution function based on the climatic information of the understudied area. Based on the electricity prices in Florida, real-time pricing (RTP) for purchasing energy carriers from the upstream grid is considered. The cost of losses, C^{loss}, in PDS and PMGs are considered equivalent to purchasing energy from the upstream grid. The energy selling price for exchanged energy between agents in the CEP is determined in the second level of the stage 1 problem. Three study cases are analyzed as follows to better illustrate the proposed CEP's benefits. The AC and DC scenarios for PDS and PMGs are considered in each case. The third case is according to the ideal resilience-oriented CEP introduced earlier.

5.1. Case I: IDSs expansion planning considering resilience

In this case study, it is assumed that the demand growth is served in existing load points, and if needed, existing lines and pipelines are reinforced. DSO owns generation and storage units and is responsible for their operation. This case study is a benchmark to investigate the effects of CEP of IDSs and MCEMs on the second and third cases. Table 6 summarizes the economic results of expansion planning of IDSs considering resilience. NPVs (in million dollars) are used to compare the cost component of the planning in IDSs, including investment, operation, resilience, and energy exchange costs. Table 7 compares AC and DC solutions for PDS. According to Tables 6 and 7, the NPV costs of losses and resilience are reduced by 32.2% and 2.2% with DC-PDS, respectively. The main reason for developing P2G in the PDS is the reduction of operating costs due to converting power to gas when power is cheap in the PDS and sale to the GDS in the hours when gas is expensive.

The sum of AC-PDS planning costs, including investment and operation, C^{CEP}, and resilience costs, C^{Re}, is 9.2% lower than DC-PDS while the coordinated expansion planning costs of IDSs with AC-PDS is 1.5% lower than IDSs with DC-PDS. Considering that the DC-PDS has to be connected to the upstream AC grid and AC generation sources like CHP, the VSC station is required, which increases investment and maintenance costs and adds some power losses. Since there is less expansion of CHP sources in DC-PDS, the cost of natural gas fuel has decreased, reducing GDS's income. Considering the load's power factor in AC-PDS and using the DC operating voltage 1.414 times the AC voltage, DC line power capacity transfer has increased by 49.7% compared to

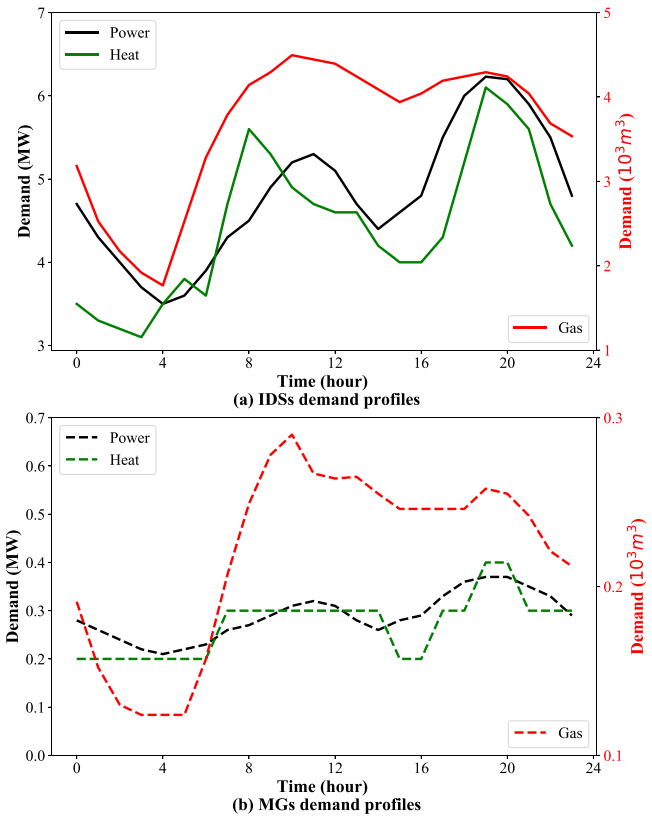

Fig. 4. Demand profiles of the IDSs (Saravi et al., 2022) and MCEMs.

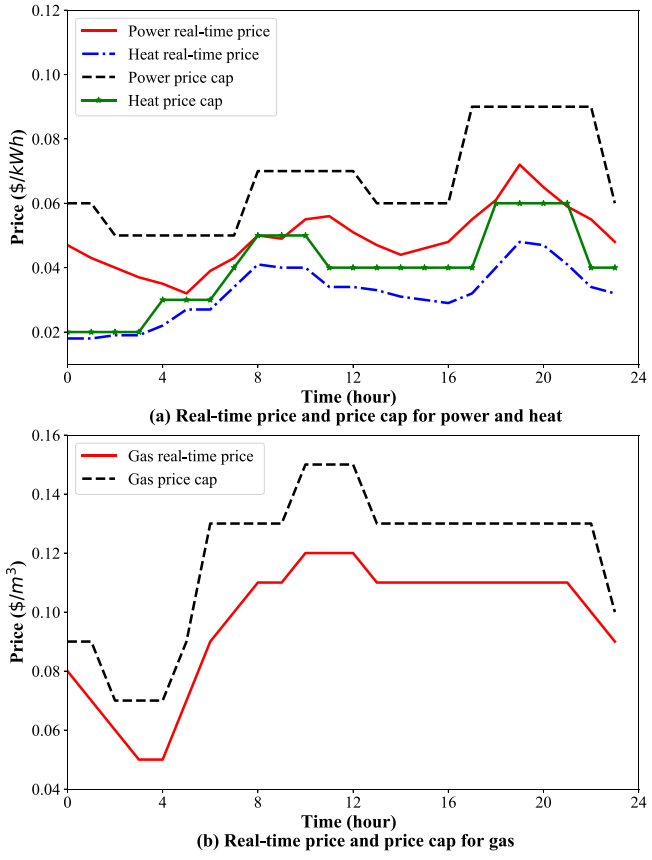

Fig. 5. The energy purchasing price from upstream grids and price cap.

Table 6
Economic results of Case I.

Network	NPV (M$)					
	AC-PDS			DC-PDS		
	C^{CEP}	C^{Re}	C^{Pr}	C^{CEP}	C^{Re}	C^{Pr}
PDS	4.481	0.249	–	4.923	0.243	–
GDS	3.643	0.018	–	3.521	0.018	–
DHS	3.973	0.009	–	3.845	0.009	–
IDSs	12.097	0.276	–	12.289	0.270	–

Table 7
Comparison between the AC and DC Solution in Case I.

Case	AC-PDS	DC-PDS	NPV (M$)		
			Losses	C^{Inv}	C^{Op}
1	☑	☐	0.223	1.314	3.167
2	☐	☑	0.151	1.701	3.222

AC, on average. Therefore, by increasing the planning horizon from 5 to 10 years, DC-PDS became the optimal configuration because lines number 1, 2, 5, 6, 19, 20, and 21 in the AC-PDS need to be reinforced, which increases the investment cost in the AC-PDS compared to DC-PDS. Another point that has a significant impact on determining the optimal configuration is the loss cost calculation method. In this paper, two scenarios for loss cost calculation are defined. In the first scenario, the real-time prices of purchasing energy from the upstream grid are used to calculate the power loss cost. The equivalent MVA losses are used to calculate power loss costs in AC-PDS. In the second scenario, according to some literature, the cost of each kilowatt of losses is considered to be equal to the average expense of 1 kilowatt of power generation in that network, revealing that, for this scenario, the net present value of CCEP in the ACPDS and DC-PDS will be equal to 5.728 M$ and 5.589 M$, respectively. Therefore, DC-PDS will be the optimal solution. Therefore, DC-PDS will be the optimal solution.

5.2. Case II: CEP without resilience

The penetration of distributed generation and the falling cost of these technologies have resulted in the rapid growth of MGs in distribution systems in recent years. Thus, as a reasonable assumption, the demand growth is served in privately owned grid-connected MGs in this case study. The coordinated expansion planning of IDSs and MCEMs with separate owners is investigated. DSO and MGSO are the operators of IDSs and MCMEs, respectively. Each of the IDSs and MCEMs has its separate owners/operators. The economic results of Case II are summarized in Table 8. Resilience is not considered in the planning problem in this case study. The resilience costs presented in Table 8 only show the costs of demand interruption and VoLL without considering resilience improvement measurements at the third level of the problem. According to Table 9, by considering the PDS planning costs independently, the AC-PDS with 5.055 M$ compared to 5.117 M$ for the DC-PDS is the optimum configuration. In contrast, in coordinated expansion planning of IDSs, the DC-PDS would become the optimal configuration with 12.618 M$ compared to 12.629 M$ for AC-PDS. The main reason is the installation of BESS in the DC-PDS instead of CHP. Due to the lower power losses and the elimination of reactive power, it is possible to develop fewer generation sources. Instead, the development of CHP resources in PMGs provides the thermal energy needs well, so considering the CEP of IDSs and MCEMs, the costs are reduced in the DC-PDS with DC-PMGs network. Table 9 compares AC, DC, and hybrid solutions for PDS and PMGs. As can be seen in Table 9, the DC-PDS with the DC-PMGs reduces the costs of losses by 56.8% compared to AC-PDS with AC-PMGs.

The negative values for MCEMs in Table 8 represent the total income from selling energy to IDSs. Based on the obtained results,

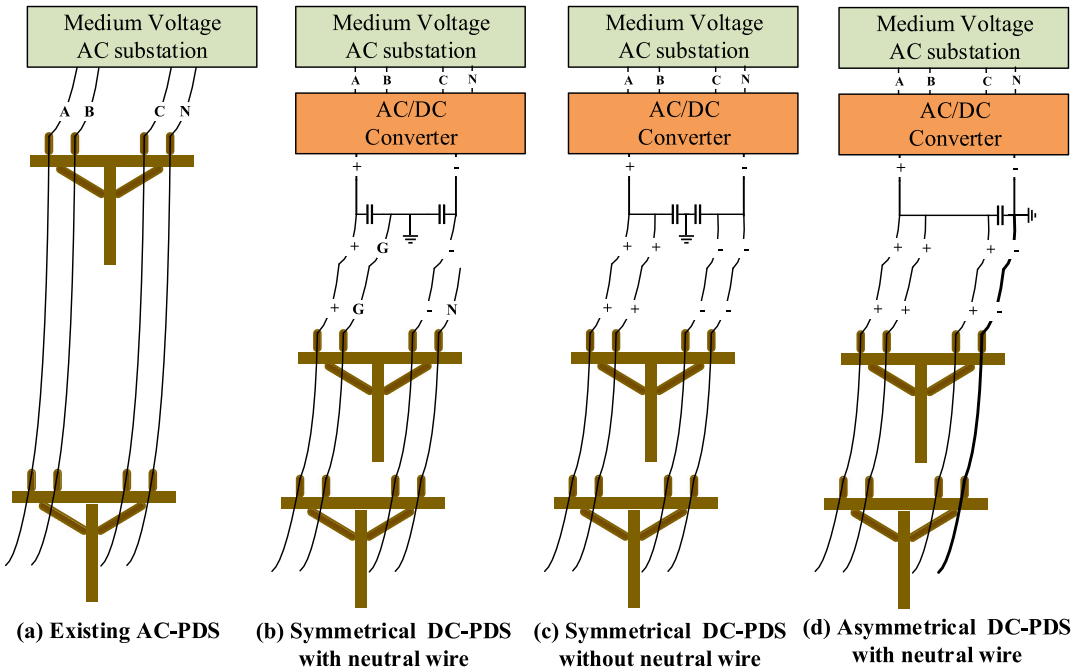

Fig. 6. Demand profiles of the IDSs (Saravi et al., 2022) and MCEMs.

Table 8
Economic results of Case II.

Network	NPV (M$)					
	AC-PDS			DC-PDS		
	C^{CEP}	C^{Re}	C^{Pr}	C^{CEP}	C^{Re}	C^{Pr}
PDS	2.658	1.106	1.291	2.898	1.020	1.199
GDS	2.311	0.131	1.178	2.278	0.127	1.242
DHS	2.973	0.168	0.813	2.977	0.161	0.716
PMG1	0.691	–	−0.610	0.738	–	−0.502
PMG2	0.751	–	−0.681	0.833	–	−0.697
GMG1	0.877	–	−0.645	1.097	–	−0.689
GMG2	0.741	–	−0.533	0.989	–	−0.553
HMG1	0.583	–	−0.388	0.620	–	−0.330
HMG2	0.601	–	−0.425	0.741	–	−0.386
IDSs	7.942	1.405	3.282	8.153	1.308	3.157

Table 9
Comparison between the AC and DC Solution in Case II.

Case	AC-PDS	DC-PDS	AC-PMGs	DC-PMGs	NPV (M$)					
					PDS			PMGs		
					Losses	C^{Inv}	C^{Op}	Losses	C^{Inv}	C^{Op}
1	☑	☐	☑	☐	0.138	0.994	1.664	0.008	0.823	0.619
2	☑	☐	☐	☑	0.138	0.994	1.664	0.005	0.926	0.672
3	☐	☑	☑	☐	0.058	1.291	1.609	0.009	0.908	0.709
4	☐	☑	☐	☑	0.058	1.291	1.607	0.005	0.869	0.702

the owners of PMG1 and PMG2 can compensate 88.2% and 90.6% of their total costs in 5 years of planning by investing in the expansion of generation in their MGs and only through the selling of excess energy to the PDS. Like case I, by increasing the planning horizon from 5 to 10 years, DC-PDS became the optimal configuration since using the chosen configuration in DC-PDS, the maximum power transfer capacity of power lines increases up to 1.587 times that of the AC-PDS. Therefore, the reinforcements of power lines are deferral in 10 years of planning in DC-PDS. Also, DC-PDS became the optimal solution by considering the cost of each kilowatt of losses to be equal to the average expense of 1 kilowatt of power generation in that network. The total NPV of power losses increases from 0.138 M$ to 0.876 M$ in AC-PDS while it becomes 0.360 M$ in DC-PDS.

5.3. Case III: CEP with resilience

The planning results offered by the CEP, considering resilience in Case III, are displayed in Table 10. This case incurs a higher investment cost due to implementing a proactive planning technique that accounts for the system's resilience in the planning problem. This approach is more conservative, resulting in increased costs for both the IDS and MCEMs. It implies that the sum of the imposed cost to the IDS and MCEMs due to the damage of poles and conductors, energy not supplied, and VoLL reduced by 72% using proactive CEP. The optimum PDS and PMGs configuration is the AC-PDS with AC-PMGs extracted from the results in Table 11 since the total NPV for CEP of IDS with DC-PDS and DC-PMGs increases by 0.4% due to the cost of building

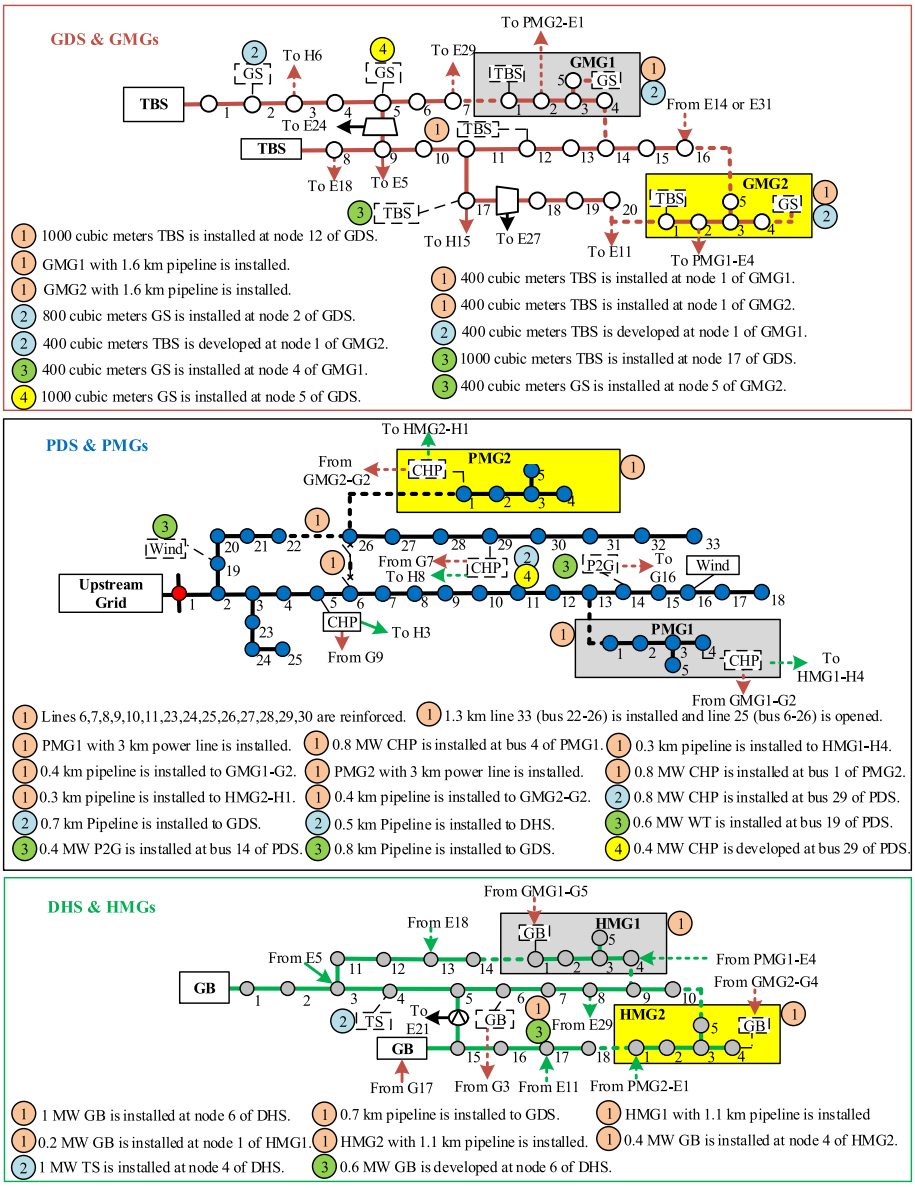

Fig. 7. The CEP results for Case III with AC-PDS.

VSCs. However, using the DC-PDS will significantly reduce the costs of losses and improve the system's resilience. According to a sensitivity analysis on the optimum configuration of PDS with changing the AC-DC power conversion costs, an 18.2% reduction in the VSCs cost will lead to changing the optimal PDS configuration from AC to DC. In summary, the optimal solution is the AC-PDS with AC-PMGs in Case III. The CEP in Case III reduces the planning costs by 0.7% compared to Case I. Also, the CEP considering resilience in Case III reduces costs by 2.7% compared to the optimum solution in Case II. Iteration process output results of the Algorithm for case III are illustrated in Figs. 7 and 8 for AC-PDS and DC-PDS, respectively. These figures show the IDS's expansion planning output in the study lifetime. Fig. 9 to Fig. 13 are provided to show more details of the study results.

According to Figs. 7 and 8, due to the significant impact of the reinforcement of vulnerable power lines in reducing resilience costs, these lines have been reinforced in both AC and DC structures in the first year. The voltage profile is improved by reconfiguring the PDS by installing line 33 and opening line 25. The generation expansion deferral is achieved at the expanse of the negligible cost of the 1.3 km power line installation. The development of PMGs in the first year has reduced the costs of the PDS, and at the same time, due to the sale of the surplus energy of PMGs to the PDSs, the cost of developing them is returned in an acceptable time. Due to the sale of heating energy from CHP sources to the HMGs by the PMGs, the development of these sources in PMGs in the first year has been the optimal scenario compared to other sources. For the same reason, and considering the coupling between PDS and DHS, the development of 0.8 MW of CHP source in both AC and DC configuration of PDS has been the optimal option.

In the third year, due to the lack of need for further development of CHP resources in the DHS and also the lower cost of BESS development in the DC-PDS, the optimal option is to install 0.6 MW of BESS, while for the AC-PDS, installing 0.6 MW of WT is the optimal option. The expansion results in the fourth year have been the same for both AC-PDS and DC-PDS. Still, in the fifth year, considering the configuration of the DC-PDS in emergency conditions, installing tie-line 5 with a length of 1.2 km will reduce the load shedding and the cost of lost load. GMG1 and GMG2 connected to the GDS, and HMG1 and HMG2 connected to the DHS have been developed in the first year of planning. Table 12 is a comparative table of total CEP costs for the case studies

Table 10
Economic results of Case III.

Network	NPV (M$)					
	AC-PDS			DC-PDS		
	C^{CEP}	C^{Re}	C^{Pr}	C^{CEP}	C^{Re}	C^{Pr}
PDS	2.718	0.283	1.422	3.045	0.244	1.398
GDS	2.364	0.047	1.204	2.350	0.047	1.271
DHS	3.178	0.063	1.006	3.134	0.063	0.778
PMG1	0.714	–	−0.607	0.753	–	−0.572
PMG2	0.723	–	−0.815	0.826	–	−0.826
GMG1	0.992	–	−0.671	1.143	–	−0.718
GMG2	0.741	–	−0.533	0.989	–	−0.553
HMG1	0.631	–	−0.495	0.611	–	−0.342
HMG2	0.662	–	−0.511	0.744	–	−0.436
IDSs	8.260	0.393	3.632	8.529	0.354	3.447

Table 11
Comparison between the AC and DC Solution in Case III.

Case	AC-PDS	DC-PDS	AC-PMGs	DC-PMGs	NPV (M$)					
					PDS			PMGs		
					Losses	C^{Inv}	C^{Op}	Losses	C^{Inv}	C^{Op}
1	☑	☐	☑	☐	0.144	1.129	1.589	0.009	0.822	0.615
2	☑	☐	☐	☑	0.144	1.129	1.830	0.006	0.938	0.724
3	☐	☑	☑	☐	0.062	1.455	1.868	0.010	0.892	0.710
4	☐	☑	☐	☑	0.062	1.455	1.590	0.005	0.881	0.698

Table 12
Comparison of case study's economic results for AC and DC configurations.

Case	Loss scenario	NPV of total CEP costs (M$)		
		AC	DC	Optimal
1	1	12.373	12.559	AC
1	2	13.620	13.225	DC
2	1	12.629	12.618	DC
2	2	13.409	12.946	DC
3	1	12.285	12.330	AC
3	2	13.103	12.678	DC

in AC and DC configurations. Here, AC configuration refers to the combination of AC-PDS and AC-PMGs, and DC configuration refers to the combination of DC-PDS and DC-PMGs. In this table, column two indicates the loss calculation scenario according to the definition in Section 5.1. The last column of the table represents the optimal configuration based on the lowest planning cost in each case. The last column of the table represents the optimal configuration based on the lowest CEP costs in each case. According to the results of Table 12, the optimal case is related to case 3 and scenario 1 for loss calculation with AC configuration. In case 2, where resilience is not considered in the CEP, its incurred costs have been significant. Considering the impact of DC configuration in reducing these costs, the optimal configuration for both loss calculation scenarios is DC configuration. The voltage profile of PDS's normal condition for case III is given in Fig. 9. This figure reveals the voltage profiles of PDS buses for the base case and years 1 and 5 of planning in the maximum demand hour, 19:00, which confirms that the DC-PDS can improve the voltage profile.

To conduct a more comprehensive analysis of the impacts of AC and DC configurations on the power losses of the PDS, Fig. 10 is presented. By eliminating reactive power flow, increasing the operating voltage of the system, and utilizing DC lines with smaller resistance compared to AC lines, the DC configuration offers notable advantages in terms of minimizing power losses.

Fig. 11 depicts the impacts of installing line 33 connecting bus 22 to bus 26 and opening the switches of line 25 connecting bus 6 to bus 26 on voltage profiles. As can be seen, voltage profiles in both the AC and DC configurations improve in the PDS and PMGs by installing this line.

Fig. 12 represents the resilience curve of the system in case studies with AC and DC configuration for the PDS. The RI in the resilience-oriented CEP of Case III with the AC-PDS configuration improves by 20.1% compared to Case II with AC-PDS, which depicts the impact of considering resilience in the planning problem. The DC configuration in Case III improves resilience by 0.7% compared to AC-PDS. The optimal energy exchange prices between IDSs and MCEMs, which MGs offer IDSs at the second level of the CEP, are illustrated in Fig. 13. According to the needs of the IDSs, PMG2, HMG2, and GMG1 are sold and purchased at price cap energy to the IDSs in more hours at the price cap compared to PMG1, HMG1, and GMG2.

Fig. 14 illustrates the power exchange profile between PMGs and the PDS in the fifth year of case III. As shown in the figure, in both AC and DC configurations, due to the optimal pricing for power exchange between PMGs and the PDS, PMGs send their surplus power to the PDS during all hours of the day, which helps to meet the load near the consumption and reduce the power losses. However, in DC configuration, for PMG1, considering the development of the BESS in bus 18, which is located near PMG1 in terms of electricity distance, and also taking into account that the energy purchase price from the microgrid during the hours of 18 to 22 is at its cap price, power exchange from PMG1 to the PDS has decreased during these hours.

The relative error of the solutions has been calculated using Eq. (14) to study the proposed algorithm's efficiency and convergence performance. To obtain the ground truth solution, $OF^{\star}$, for measuring the relative errors in the solutions, 2000 iterations with a conservative approach run. The obtained results are considered the optimum solutions. The convergence rate in reaching the relative error equal to 0.001 for the LADMMPSAP method in Saravi et al. (2022) and the proposed ADP-LADMMPSAP algorithm are compared for Case III with AC-PDS, as shown in Fig. 15. The convergence speed in the proposed algorithm has increased significantly, indicating its efficiency for complex problems.

$$Error = \frac{|OF - OF^{\star}|}{OF^{\star}} \tag{14}$$

6. Conclusion

This paper proposed a three-level, two-stage coordinated stochastic expansion planning of IDSs and MCEMs, considering resilience for determining the technologies, capacities, and location of components and MGs in the IDSs integrated with MCEMs. The proposed model considered AC and DC configuration for PDS and could offer informative reference to the distribution system planners. The model properly

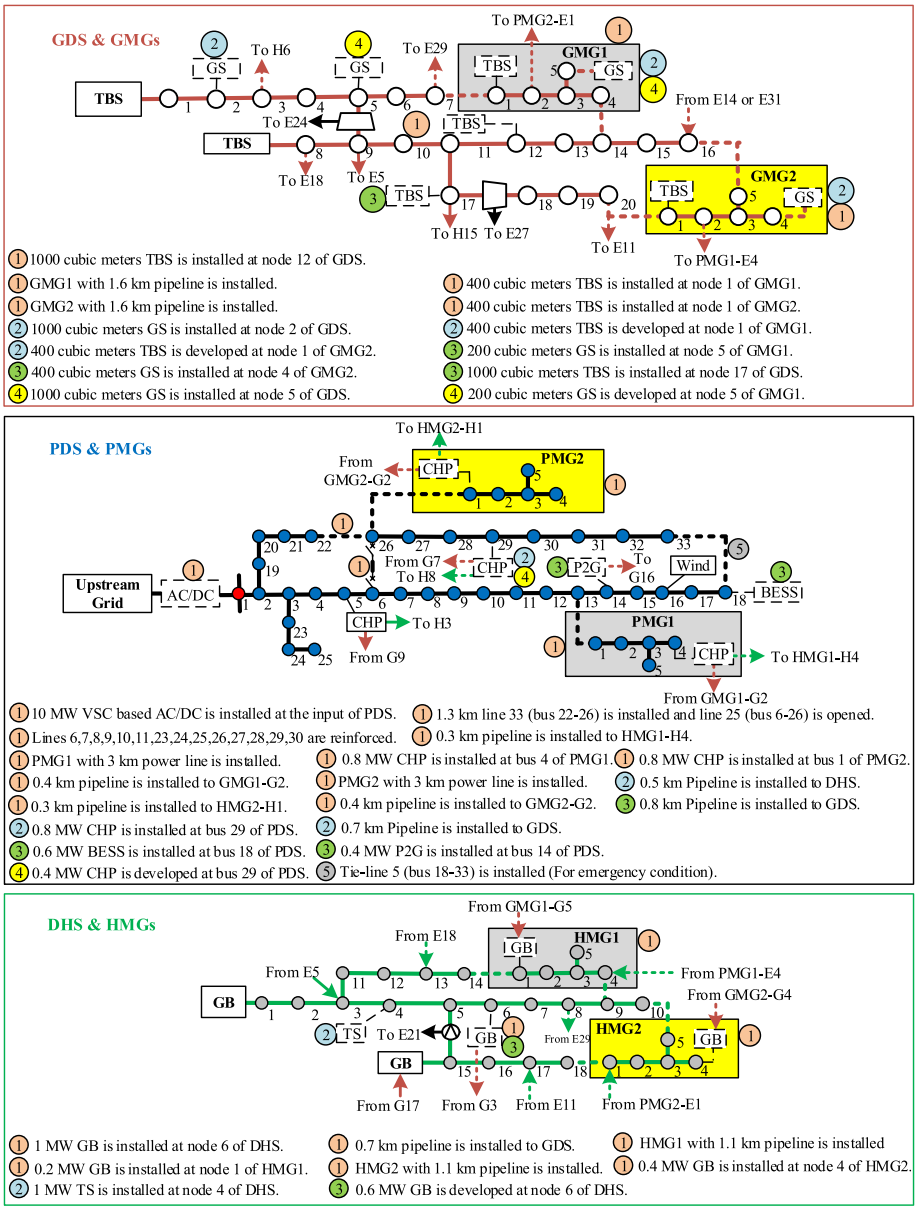

Fig. 8. The CEP results for Case III with DC-PDS.

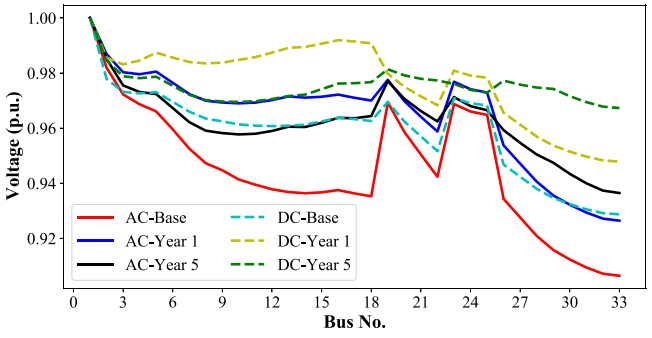

Fig. 9. Voltage profiles in normal condition of Case III.

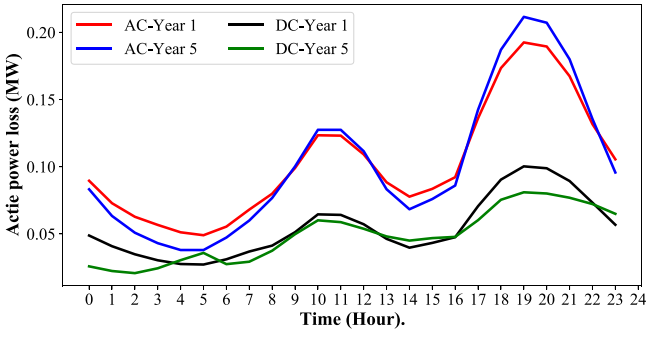

Fig. 10. Final iteration process result for case III with AC-PDS.

considered operating and resilience requirements and energy exchange profit of MCEMs with the optimal price and the amount of exchange energy. An aggregator-splitting approach using the ACC was introduced, significantly reducing the problem's computational complexity. The following implications were delivered from case studies: The coordinated planning could reduce the IDSs costs through the system's expansion by independent MCEMs. In Case III, the investment costs in MGs are returned in the planning period without considering the income from energy sales to final consumers and only through the sale of energy to the IDSs. In 5-year planning, AC and DC configuration costs are close,

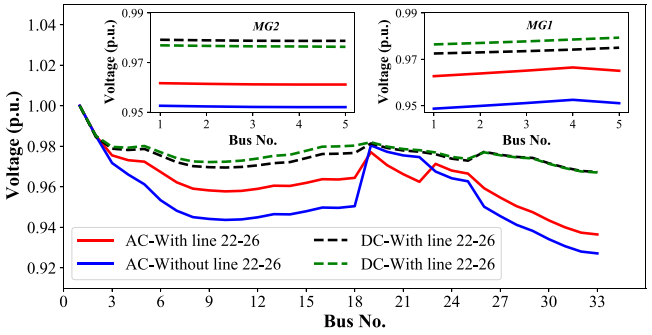

Fig. 11. Final iteration process result for case III with DC-PDS.

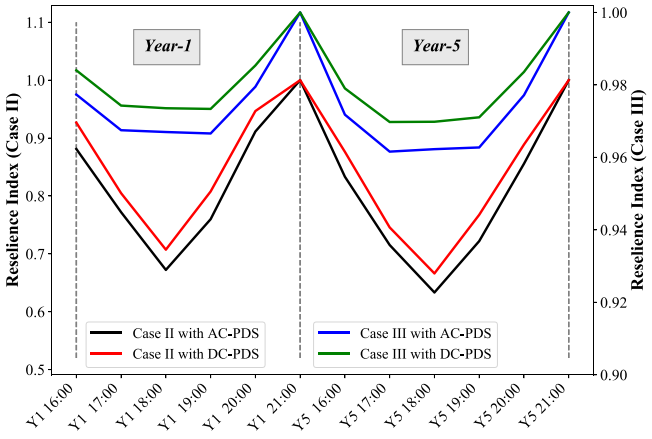

Fig. 12. Resilience Index of the IDSs in case studies.

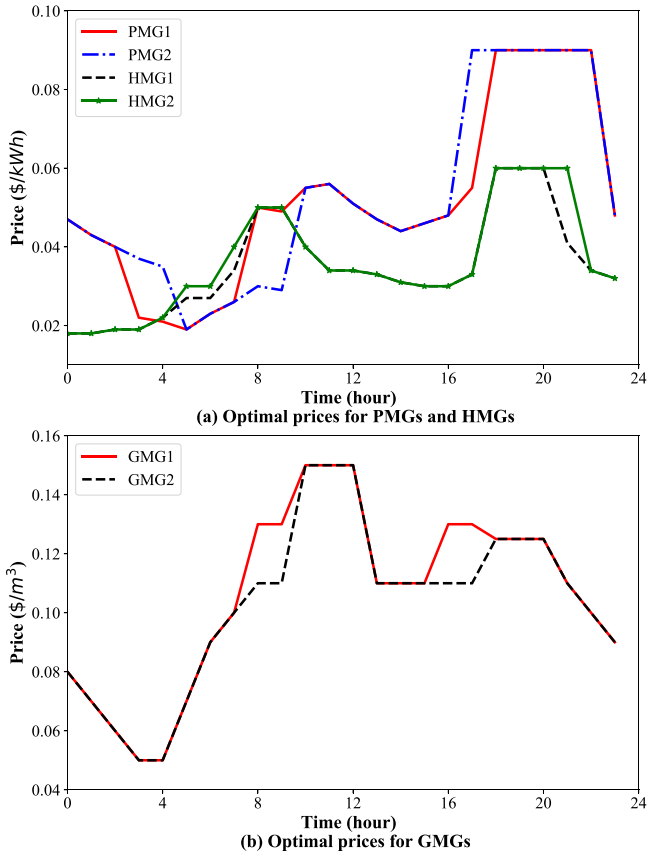

Fig. 13. Optimal energy exchange prices in second level problem.

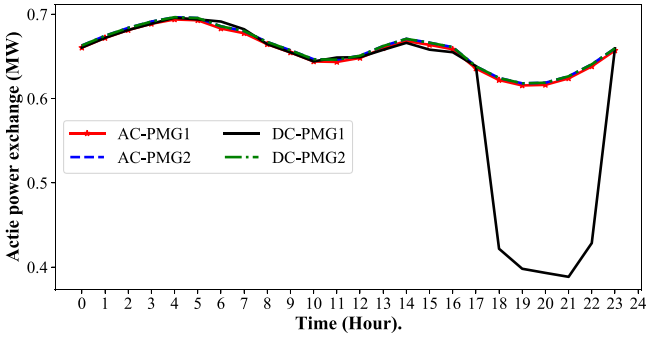

Fig. 14. Active power exchange of PMGs with PDS in year 5 of Case III.

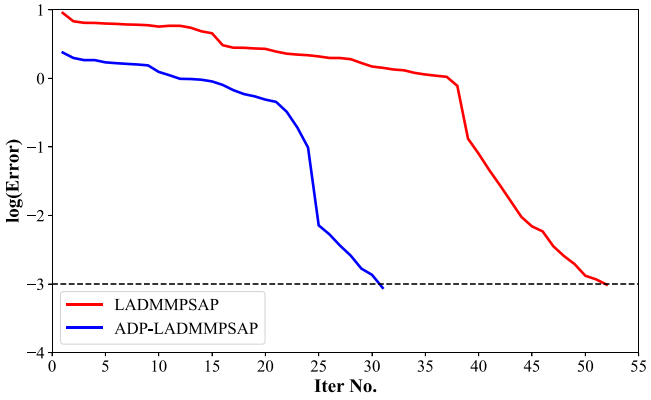

Fig. 15. Convergence curve of Case III with AC-PDS.

and the AC is the optimal choice in all case studies. By increasing the planning horizon to 10 years, DC will be the optimal solution since network reinforcement costs and power losses are significantly lower. Also, suppose the value of losses is equal to the average cost of one kilowatt of power generation in the PDS; DC will be the optimal option. In that case, DC will be the superior option in all the case studies. Comparing Case II and III, despite the increase in investment cost, considering resilience in planning, overall network costs will decrease by 2.7% during the planning period. From the investment tendency point of view, with the continuous drop of VSC building costs and the increased penetration of BESS, the DC configuration will be the inevitable option for future PDSs. It is worth mentioning that the MG's operation was considered autonomous, and collaboration between MGs using making a coalition is not considered in this paper. This is the topic of the author's future work.

Declaration of competing interest

The authors declare that they have no known competing financial interests or personal relationships that could have appeared to influence the work reported in this paper.

Data availability

Data will be made available on request.

Acknowledgments

Amjad Anvari-Moghaddam acknowledges the support of the "MARGIN–Market-driven Multi-Energy Operational Planning in Indonesia" project funded by the Danida Fellowship Centre and the Ministry of Foreign Affairs of Denmark to research in growth and transition countries under the grant no. 21-M06-AAU.

Table A.1
Simulation parameters.

Parameter	Value	Parameter	Value
$\underline{CR}, \overline{CR}$	1,1.2	$\zeta_{5,9}, \zeta_{17,18}$	1.08,1.12
$\overline{S}^{Imp}$	10 MVA	$\varepsilon_1, \varepsilon_2$	0.001
$\underline{V}_i, \overline{V}_i$	0.9,1.1 p.u.	μ^0, ρ_0	2,0.01
P^f_{Th}	0.1	μ^{max}	100
τ^a	25^{oC}	$C^{LL}_{PDS}, C^{LL}_{PMG}$	25 $/kWh
$C^{LL}_{HDS}, C^{LL}_{HMG}$	10 $/kWh	$C^{LL}_{GDS}, C^{LL}_{GMG}$	15 $/kWh
$\underline{SOC}, \overline{SOC}$	0.1,0.9	Gas heating value	250 kW/m^3

Table A.2
PMGs buses geographical coordination.

Network	Bus No.	Coordinate (longitude, latitude)
PMG1	1	(82.6100W, 28.0550N)
	2	(82.6050W, 28.0550N)
	3	(82.6010W, 28.0550N)
	4	(82.5790W, 28.0550N)
	5	(82.6010W, 28.05300N)
PMG2	1	(82.6610W, 28.0680N)
	2	(82.6570W, 28.0680N)
	3	(82.6530W, 28.0680N)
	4	(82.6490W, 28.0680N)
	5	(82.6530W, 28.0710N)
PMG2	1	(82.7670W, 28.0840N)
	2	(82.7620W, 28.0840N)
	3	(82.7580W, 28.0840N)
	4	(82.7540W, 28.0840N)
	5	(82.7580W, 28.0810N)

Table A.3
Data of interconnected lines and pipelines.

Type	Network (from–to)	Bus\node no.	Length (km)
Pipeline	GMG1-PMG1	2–4	0.2
Pipeline	PMG1-HMG1	4–4	0.1
Pipeline	GMG1-HMG1	5–1	0.3
Pipeline	GMG2-PMG2	2–1	0.2
Pipeline	PMG2-HMG2	1–1	0.2
Pipeline	GMG2-HMG2	4–4	0.1
Pipeline	GMG3-PMG3	2–5	0.3
Pipeline	PMG3-HMG3	5–4	0.2
Pipeline	GMG3-HMG3	3–1	0.3

Table A.4
Data of MGs lines and pipelines.

Network	Lines\pipelines of MGs			Candidate interconnection		
	Line No.	Line(i–j)	Length (km)	Line No.	Line (i–j) (MGs to IDSs)	Length (km)
PMGs	1	1–2	0.5	5	1–26	1
	2	2–3	0.4	6	4–33	0.8
	3	3–4	0.4	5	1–13	1
	4	3–5	0.3	6	4–18	0.8
				5	4–23	0.7
GMGs	1	1–2	0.2	5	1–7	0.4
	2	2–3	0.2	6	4–14	0.5
	3	3–4	0.3	5	1–20	0.5
	4	3–5	0.3	6	5–16	0.4
				5	5–2	0.6
HMGs	1	1–2	0.1	5	1–14	0.3
	2	2–3	0.2	6	4–9	0.2
	3	3–4	0.2	5	1–18	0.2
	4	3–5	0.2	6	5–10	0.3
				5	5–3	0.4

Appendix. Data and simulation parameters

Technical data of IDSs and MCEMs, including the PDS's pole classes, PMGs line data, couplings of IDSs and MCEMs, and simulation parameters, are given in Tables A.1–A.4.

References

Adnan, M., Khan, M. G., Amin, A. A., Fazal, M. R., Tan, W.-S., & Ali, M. (2021). Cascading failures assessment in renewable integrated power grids under multiple faults contingencies. *IEEE Access*, *9*, 82272–82287.

Ahmed, H. M. A., Eltantawy, A. B., & Salama, M. M. A. (2018). A planning approach for the network configuration of AC-DC hybrid distribution systems. *IEEE Transactions*

on Smart Grid, *9*(3), 2203–2213.
Al-Ismail, F. S. (2021). DC microgrid planning, operation, and control: A comprehensive review. *IEEE Access*, *9*, 36154–36172.
Amirioun, M. H., Aminifar, F., & Shahidehpour, M. (2019). Resilience-promoting proactive scheduling against hurricanes in multiple energy carrier microgrids. *IEEE Transactions on Power Systems*, *34*(3), 2160–2168.
Arif, A., Ma, S., Wang, Z., Wang, J., Ryan, S. M., & Chen, C. (2018). Optimizing service restoration in distribution systems with uncertain repair time and demand. *IEEE Transactions on Power Systems*, *33*(6), 6828–6838.
Bao, M., Ding, Y., Sang, M., Li, D., Shao, C., & Yan, J. (2020). Modeling and evaluating nodal resilience of multi-energy systems under windstorms. *Applied Energy*, *270*, Article 115136.
Behzadi, S., & Bagheri, A. (2023). A convex micro-grid-based optimization model for planning of resilient and sustainable distribution systems considering feeders routing and siting/sizing of substations and DG units. *Sustainable Cities and Society*, *97*, Article 104787.
Dragicevic, T., Wheeler, P., & Blaabjerg, F. (2018). *Energy engineering*, *DC distribution systems and microgrids*. Institution of Engineering and Technology.
Faramarzi, D., Rastegar, H., Riahy, G., & Doagou-Mojarrad, H. (2023). A three-stage hybrid stochastic/IGDT framework for resilience-oriented distribution network planning. *International Journal of Electrical Power & Energy Systems*, *146*, Article 108738.
Geidl, M., & Andersson, G. (2007). Optimal power flow of multiple energy carriers. *IEEE Transactions on Power Systems*, *22*(1), 145–155.
Gharehveran, S. S., Ghassemzadeh, S., & Rostami, N. (2022). Two-stage resilience-constrained planning of coupled multi-energy microgrids in the presence of battery energy storages. *Sustainable Cities and Society*, *83*, Article 103952.
Good, N., & Mancarella, P. (2019). Flexibility in multi-energy communities with electrical and thermal storage: A stochastic, robust approach for multi-service demand response. *IEEE Transactions on Smart Grid*, *10*(1), 503–513.
Guo, Z., Li, G., Zhou, M., & Feng, W. (2019). Resilient configuration approach of integrated community energy system considering integrated demand response under uncertainty. *IEEE Access*, *7*, 87513–87533.
Habibifar, R., Khoshjahan, M., Saravi, V. S., & Kalantar, M. (2021). Robust energy management of residential energy hubs integrated with Power-to-X technology. In *2021 IEEE Texas power and energy conference* (pp. 1–6).
He, L., Ishibuchi, H., Trivedi, A., Wang, H., Nan, Y., & Srinivasan, D. (2021). A survey of normalization methods in multiobjective evolutionary algorithms. *IEEE Transactions on Evolutionary Computation*, *25*(6), 1028–1048.
He, C., Wu, L., Liu, T., & Bie, Z. (2018). Robust co-optimization planning of inter-dependent electricity and natural gas systems with a joint N-1 and probabilistic reliability criterion. *IEEE Transactions on Power Systems*, *33*(2), 2140–2154.
Hemmati, R., Mehrjerdi, H., & Nosratabadi, S. M. (2021). Resilience-oriented adaptable microgrid formation in integrated electricity-gas system with deployment of multiple energy hubs. *Sustainable Cities and Society*, *71*, Article 102946.
Huang, W., Zhang, N., Yang, J., Wang, Y., & Kang, C. (2019). Optimal configuration planning of multi-energy systems considering distributed renewable energy. *IEEE Transactions on Smart Grid*, *10*(2), 1452–1464.
Jithin, K., Haridev, P. P., Mayadevi, N., Kumar, R. H., & Mini, V. P. (2022). A review on challenges in DC microgrid planning and implementation. *Journal of Modern Power Systems and Clean Energy*, 1–21.
Khaligh, V., & Anvari-Moghaddam, A. (2019). Stochastic expansion planning of gas and electricity networks: A decentralized-based approach. *Energy*, *186*, Article 115889.
Krause, T., Andersson, G., Fröhlich, K., & Vaccaro, A. (2011). Multiple-energy carriers: Modeling of production, delivery, and consumption. *Proceedings of the IEEE*, *99*(1), 15–27.
Li, Z., Wu, W., Shahidehpour, M., Wang, J., & Zhang, B. (2016). Combined heat and power dispatch considering pipeline energy storage of district heating network. *IEEE Transactions on Sustainable Energy*, *7*(1), 12–22.
Li, G., Zhang, R., Jiang, T., Chen, H., Bai, L., Cui, H., & Li, X. (2017). Optimal dispatch strategy for integrated energy systems with CCHP and wind power. *Applied Energy*, *192*, 408–419.
Liu, P., Ding, T., Zou, Z., & Yang, Y. (2019). Integrated demand response for a load serving entity in multi-energy market considering network constraints. *Applied Energy*, *250*, 512–529.
Liu, X., & Mancarella, P. (2016). Modelling, assessment and sankey diagrams of integrated electricity-heat-gas networks in multi-vector district energy systems. *Applied Energy*, *167*, 336–352.
Liu, P., Wu, Z., Gu, W., Lu, Y., Yang, X., Sun, K., & Sun, Q. (2022). Security-constrained AC–DC hybrid distribution system expansion planning with high penetration of renewable energy. *International Journal of Electrical Power & Energy Systems*, *142*, Article 108285.
Liu, Y., Yao, W., Zhou, X., Zhou, Q., Li, C., & Gong, J. (2021). Optimal planning of park integrated energy system considering the resilience of distribution network. In *2021 IEEE 5th conference on energy internet and energy system integration* (pp. 1680–1685).
Mancarella, P. (2014). MES (multi-energy systems): An overview of concepts and evaluation models. *Energy*, *65*, 1–17.
Mansour-Saatloo, A., Pezhmani, Y., Mirzaei, M. A., Mohammadi-Ivatloo, B., Zare, K., Marzband, M., & Anvari-Moghaddam, A. (2021). Robust decentralized optimization of multi-microgrids integrated with Power-to-X technologies. *Applied Energy*, *304*, Article 117635.
Mirzaei, M. A., Nazari-Heris, M., Zare, K., Mohammadi-Ivatloo, B., Marzband, M., Asadi, S., & Anvari-Moghaddam, A. (2020). Evaluating the impact of multi-carrier energy storage systems in optimal operation of integrated electricity, gas and district heating networks. *Applied Thermal Engineering*, *176*, Article 115413.
Moreira, A., Strbac, G., Moreno, R., Street, A., & Konstantelos, I. (2018). A five-level MILP model for flexible transmission network planning under uncertainty: A min–max regret approach. *IEEE Transactions on Power Systems*, *33*(1), 486–501.
Najafi, J., Peiravi, A., Anvari-Moghaddam, A., & Guerrero, J. M. (2019). Resilience improvement planning of power-water distribution systems with multiple microgrids against hurricanes using clean strategies. *Journal of Cleaner Production*, *223*, 109–126.
Najafi, J., Peiravi, A., Anvari-Moghaddam, A., & Guerrero, J. (2020). An efficient interactive framework for improving resilience of power-water distribution systems with multiple privately-owned microgrids. *International Journal of Electrical Power & Energy Systems*, *116*, Article 105550.
Nourollahi, R., Zare, K., Mohammadi-Ivatloo, B., Vahidinasab, V., & Moghadam, A. A. (2023). Continuous-time optimization of integrated networks of electricity and district heating under wind power uncertainty. *Applied Thermal Engineering*, *225*, Article 119926.
Ouyang, S., Xin, X., Wang, F., Huang, Y., & Yang, M. (2022). Research on optimization strategy of urban medium voltage direct current distribution network construction considering application scenarios. *IET Generation, Transmission & Distribution*, *16*(24), 5041–5051.
Poudyal, A., Poudel, S., & Dubey, A. (2022). Risk-based active distribution system planning for resilience against extreme weather events. *IEEE Transactions on Sustainable Energy*, 1–14.
Qu, L., Yu, Z., Song, Q., Yuan, Z., Zhao, B., Yao, D., Chen, J., Liu, Y., & Zeng, R. (2022). Planning and analysis of the demonstration project of the MVDC distribution network in Zhuhai. *Frontiers in Energy*, *13*, 120–130.
Ren, F., Lin, X., Ma, X., Wei, Z., Wang, R., & Zhai, X. (2023). A two-stage planning method for design and dispatch of distributed energy networks considering multiple energy trading. *Sustainable Cities and Society*, *96*, Article 104666.
Salyani, P., Nourollahi, R., Zare, K., & Razzaghi, R. (2023). A cooperative game approach for optimal resiliency-oriented scheduling of transactive multiple microgrids. *Sustainable Cities and Society*, *89*, Article 104358.
Saravi, V. S., Kalantar, M., & Anvari-Moghaddam, A. (2022). Resilience-constrained expansion planning of integrated power–gas–heat distribution networks. *Applied Energy*, *323*, Article 119315.
Tabebordbar, A., Rastegar, M., & Ebrahimi, M. (2023). Reliability-oriented optimal sizing of power-to-gas and combined heat and power technologies in integrated electricity and natural gas transmission systems. *Sustainable Cities and Society*, *95*, Article 104593.
Tao, R., Zhao, D., Xu, C., Wang, H., & Xia, X. (2023). Resilience enhancement of integrated electricity-gas-heat urban energy system with data centres considering waste heat reuse. *IEEE Transactions on Smart Grid*, *14*(1), 183–198.
Vilaisarn, Y., Rodrigues, Y. R., Abdelaziz, M. M. A., & Cros, J. (2022). A deep learning based multiobjective optimization for the planning of resilience oriented microgrids in active distribution system. *IEEE Access*, *10*, 84330–84364.
Wang, S., & Bo, R. (2023). A resilience-oriented multi-stage adaptive distribution system planning considering multiple extreme weather events. *IEEE Transactions on Sustainable Energy*, *14*(2), 1193–1204.
Xu, Y., Ding, T., Qu, M., & Du, P. (2020). Adaptive dynamic programming for gas-power network constrained unit commitment to accommodate renewable energy with combined-cycle units. *IEEE Transactions on Sustainable Energy*, *11*(3), 2028–2039.
Xu, D., Wu, Q., Zhou, B., Li, C., Bai, L., & Huang, S. (2020). Distributed multi-energy operation of coupled electricity, heating, and natural gas networks. *IEEE Transactions on Sustainable Energy*, *11*(4), 2457–2469.
Yuan, J., Zhang, G., Yu, S. S., Chen, Z., Li, Z., & Zhang, Y. (2022). A multi-timescale smart grid energy management system based on adaptive dynamic programming and multi-NN fusion prediction method. *Knowledge-Based Systems*, *241*, Article 108284.
Zhang, X., Karady, G. G., & Ariaratnam, S. T. (2014). Optimal allocation of CHP-based distributed generation on urban energy distribution networks. *IEEE Transactions on Sustainable Energy*, *5*(1), 246–253.
Zhang, L., Liang, J., Tang, W., Li, G., Cai, Y., & Sheng, W. (2019). Converting AC distribution lines to DC to increase transfer capacities and DG penetration. *IEEE Transactions on Smart Grid*, *10*(2), 1477–1487.
Zhang, X., Shahidehpour, M., Alabdulwahab, A., & Abusorrah, A. (2015). Optimal expansion planning of energy hub with multiple energy infrastructures. *IEEE Transactions on Smart Grid*, *6*(5), 2302–2311.

Zhang, L., Tong, B., Wang, Z., Tang, W., & Shen, C. (2022). Optimal configuration of hybrid AC/DC distribution network considering the temporal power flow complementarity on lines. *IEEE Transactions on Smart Grid*, *13*(5), 3857–3866.

Zhao, X., Chen, Y., Liu, K., Xu, G., Chen, H., & Liu, W. (2023). Design and operation of park-level integrated energy systems in various climate zones in China. *Sustainable Cities and Society*, *96*, Article 104705.

Zhao, P., Gu, C., Cao, Z., Ai, Q., Xiang, Y., Ding, T., Lu, X., Chen, X., & Li, S. (2021). Water-energy nexus management for power systems. *IEEE Transactions on Power Systems*, *36*(3), 2542–2554.

Zhao, J., Xiong, J., Yu, H., Bu, Y., Zhao, K., Yan, J., Li, P., & Wang, C. (2022). Reliability evaluation of community integrated energy systems based on fault incidence matrix. *Sustainable Cities and Society*, *80*, Article 103769.